

~~CONFIDENTIAL~~

Copy 6  
RM E54I28

NACA RM E54I28



# RESEARCH MEMORANDUM

STEADY-STATE AND SURGE CHARACTERISTICS OF A COMPRESSOR

EQUIPPED WITH VARIABLE INLET GUIDE VANES

OPERATING IN A TURBOJET ENGINE

By Lewis E. Wallner and Robert J. Lubick

Lewis Flight Propulsion Laboratory  
Cleveland, Ohio

**LIBRARY COPY**

JUN 22 1955

LANGLEY AERONAUTICAL LABORATORY  
LIBRARY, NACA  
LANGLEY FIELD, VIRGINIA

CLASSIFIED DOCUMENT

This material contains information affecting the National Defense of the United States within the meaning of the espionage laws, Title 18, U.S.C., Secs. 793 and 794, the transmission or revelation of which in any manner to an unauthorized person is prohibited by law.

**NATIONAL ADVISORY COMMITTEE  
FOR AERONAUTICS**

WASHINGTON

June 20, 1955

*By authority of Major Gen. 1. E. E. E. Date 9-17-58 JSA*

CLASSIFICATION CHANGED

UNCLASSIFIED

To

~~CONFIDENTIAL~~

UNCLASSIFIED

NATIONAL ADVISORY COMMITTEE FOR AERONAUTICS

RESEARCH MEMORANDUM

STEADY-STATE AND SURGE CHARACTERISTICS OF A COMPRESSOR EQUIPPED WITH  
VARIABLE INLET GUIDE VANES OPERATING IN A TURBOJET ENGINE

By Lewis E. Wallner and Robert J. Lubick

SUMMARY

A turbojet engine with variable inlet guide vanes was investigated in an NACA altitude test facility to determine the steady-state compressor performance and surge characteristics. The compressor was instrumented with hot-wire anemometers to study compressor stall. In addition, performance parameters were recorded on oscillographs during engine fuel-flow transients. Compressor operation with the inlet guide vanes in the top-speed design or open position resulted in three regions of compressor operation: low speed, where the blade tips in the early stages were stalled; medium speed, where one rotating-stall zone existed; and high speed, where the compressor operated stall-free. Closing the inlet guide vanes eliminated the steady-state stalled region and improved the acceleration margin two- to twentyfold.

Compressor surge pressure ratios were unaffected by changes in flight condition for either position of the inlet guide vanes. However, decreasing the inlet Reynolds number reduced the corrected fuel flow required for compressor surge. Variations in the data from several engines had only a small effect on the surge pressure ratio but a sizable effect on the fuel flow required for surge.

INTRODUCTION

As a result of stage-matching difficulties, such as discussed in reference 1, many problems arise in the off-design operation of a compressor. At low speeds, rotating stalls generally exist (refs. 2 to 4), which not only hurt performance but can damage both single- and multi-stage compressors by exciting high vibrational stress levels (refs. 5 and 6). In addition, the violent surging that can be encountered during acceleration from off-design to rated operating conditions can be very dangerous. Several means for alleviating these problems have been suggested, some of which are interstage air bleed, inlet flow spoilers, and variable stators or inlet guide vanes. The effectiveness of inlet spoilers is discussed in reference 7.

The present paper is an analysis of the following experimental investigations of a current production engine with a compressor having variable-position inlet guide vanes:

- (1) Internal aerodynamic phenomena in the low-speed region where steady-state stall often exists and the high-speed region of stall-free compressor operation
- (2) Engine accelerations to determine compressor surge characteristics, amplitudes, frequencies, and reproducibility
- (3) Effects of variations in inlet-guide-vane position on compressor surge pressure ratio and engine surge fuel flow, and effects of flight condition on engine surge limits

This report presents a comprehensive examination of the internal performance of the compressor. Compressor surge limits are presented in terms of compressor pressure ratio, engine fuel flow, and engine speed. The steady-state stall operation is shown in terms of stage pressure ratios, temperature ratios, and pressure coefficients. Effects of inlet-guide-vane position and stall on over-all compressor performance are demonstrated by plots of pressure ratio as functions of speed and air flow.

The investigation was made at the NACA Lewis laboratory at simulated altitudes from 15,000 to 45,000 feet, flight Mach numbers from 0.3 to 1.2, and inlet-air temperatures from ambient to 160° F. Engine speed was varied from about 60 to 100 percent of rated speed.

#### APPARATUS

The subject turbojet engine, which is in the 9000-pound-thrust class, is shown installed in the altitude test chamber in figure 1. The 12-stage axial-flow-compressor rotor is shown in figure 2. The rotor tip diameter, which is constant for all compressor stages, is  $32\frac{1}{8}$  inches. The hub-tip radius ratio varies from 0.46 at the first stage to 0.88 at the twelfth stage. At rated engine operating conditions (7950 rpm), the sea-level performance of the compressor is as follows:

Air flow, $W$ , lb/sec . . . . .	141
Adiabatic efficiency, $\eta$ . . . . .	0.81
Pressure ratio, $P_3/P_2$ . . . . .	6.9

The compressor is equipped with variable-position inlet guide vanes to improve the off-design performance. The guide-vane assembly consists of 21 blades whose angle setting can be varied from 13° to 43°. In the

open position, the angles between the center line and the chord line at the root and the tip are  $0^{\circ}$  and  $13^{\circ}$ , respectively. When operated automatically, the guide vanes change from closed to open as the speed is increased above 6800 rpm.

The engine is also equipped with a cannular combustor, a two-stage axial-flow turbine, and a fixed-area conical exhaust nozzle. Ordinarily, the engine is controlled with a hydraulic fuel regulator; however, for the surge investigation, the automatic control was removed, and a specially designed external fuel valve was used to control the size and rate of fuel changes. No appreciable time lags were present in this fuel system.

The investigation was conducted in the test chamber of the altitude test facility schematically shown in figure 3. Air supplied to the inlet section of the altitude chamber can be either heated or refrigerated to the desired temperature. Automatic throttling valves were used to maintain the inlet and exhaust pressures at the desired level.

Instrumentation used to measure the steady-state compressor performance is indicated in figure 4. The probes on the interstage rakes, located in the stator rows, were equally spaced. The following quantities were measured on a multiple-channel oscillograph:

- (1) Compressor-inlet total pressure
- (2) Compressor-outlet total pressure
- (3) Compressor speed
- (4) Exhaust-gas temperature
- (5) Engine fuel flow
- (6) Engine-inlet dynamic pressure

In addition to this transient instrumentation, remotely actuated hot-wire anemometers were used to measure flow fluctuations in the first, fifth, and twelfth compressor stator rows. A schematic diagram of this instrumentation setup is shown in figure 5. The hot-wire anemometers were used to determine the presence, frequency, and number of rotating stalls. No attempt was made to determine the quantitative variation in internal air velocities. The probes were generally immersed about  $1/2$  inch from the outer wall, although for some running the depth was varied to determine the radial extent of the rotating stall.

## PROCEDURE

Compressor pressure ratios above steady-state equilibrium values were obtained by making rapid increases in fuel flow into the engine. Varying the size of the fuel step made possible the determination of the approximate value of fuel flow required to cause the compressor to surge. In addition, ramp changes in fuel flow, from 0.02 to 3 seconds in duration, were attempted to determine whether the fuel input rate affected the engine fuel flow required to cause surge. Both compressor pressure ratio and fuel flow at surge were found to be unaffected by fuel input rate. The fuel flow at surge was determined from oscillograph traces. The engine was operated over the complete speed range to map the location of the stall regions. In addition to pressures and temperatures throughout the compressor, which were recorded for the steady-state points, the output of the hot-wire anemometers was recorded on high-speed photographic film. Oscillograph traces were calibrated by operating the engine at several widely different operating points and recording the corresponding pen deflections on the oscillograph trace.

3494

## RESULTS AND DISCUSSION

For the investigation of the compressor characteristics, two production engines of the same model were used. During the course of the study, each engine underwent a factory tear-down for inspection. In general, engine parts that might change the aerodynamic performance of the engine were not replaced. Nevertheless, there were some quantitative differences in the compressor characteristics from engine to engine. These differences, however, probably do not alter the trends demonstrated in this study. A discussion of the magnitude of these differences is presented later. In order to understand the surge characteristics of the engine, it is first necessary to understand the steady-state behavior of the compressor.

## Compressor Performance

Types of steady-state operation. - The stall characteristics of the compressor during steady-state operation with the inlet guide vanes in the open position are shown in figures 6 to 8. Outputs of hot-wire-anemometer probes (which reflect  $\rho V$  variations) in the first, fifth and twelfth stator rows are presented in figure 6 for stall-free operation, rotating stall, and tip stall. During stall-free compressor operation, the traces of the hot-wire anemometers indicate high-frequency random fluctuations (fig 6(a)). As compressor speed is reduced, rotating stall is encountered (figs. 6(b) and (c)). (A discussion of rotating stall can be found in ref. 2.)

From these anemometer probes it was found that a single stalled region existed axially throughout the compressor. Generally, the rotating-stall inception was noted simultaneously on all the anemometer probes. By moving the anemometer probes radially toward the hub, it was found that the intensity of the rotating stall diminished. At about midpassage, flow irregularities were no longer perceptible. Rotating-stall operation nearest design speed (fig. 6(b)) has a smaller stalled portion of a given cycle than that occurring further from design speed (fig. 6(c)). Further reduction in compressor speed results in stall of the compressor blade tips without intermittent recovery, hereafter referred to as tip stall (fig. 6(d)). Oscillograph traces in tip stall are low-frequency (compared with stall-free operation), random amplitude fluctuations.

The time-integrated radial temperature and pressure distributions across a flow passage in the fourth stator stage (fig. 7) demonstrate that the flow disturbances during steady-state stall are near the blade tips. During tip-stall operation, the temperatures and pressures at the outer wall were 15 percent higher and 8 percent lower, respectively, than those at the hub. The anemometer probes also indicated disappearance of the tip stall at about the midpassage as they were moved radially toward the hub.

The speed range over which the various types of compressor operation occur is demonstrated in figure 8 for operation with open inlet guide vanes. The ratio of tip to average interstage temperature is relatively high during tip stall as compared with stall-free operation. The effect of tip stall is more predominant in the early stages, as evidenced by the decreasing temperature ratios after the fourth stage. Tip stall also disappeared in the latter stages of another compressor design in reference 8.

Rotating stall is effectively a transitional state between tip stall (low engine speeds) and stall-free operation (high engine speeds). At an engine speed of about 5700 rpm, where rotating stall is first encountered, the temperature ratios are almost the same as those in tip stall; at about 6500 rpm, where the stalled portion of the compressor circumference is small, the temperature ratios are close to those during stall-free operation. The same general trends are indicated by the tip-to-average pressure ratios in figure 8(b) for the fourth stator stage, and the compressor efficiency plot in figure 8(c). During tip stall, compressor efficiency is as much as 20 percent lower than rated-speed efficiency. The overlap in engine speed for each type of operation shown on these plots is a hysteresis effect. For instance, when increasing engine speed in rotating stall, this mode of compressor operation will continue to a speed of about 6550 rpm. However, when decreasing speed from stall-free operation, rotating stall would not be

obtained until a speed of approximately 6100 rpm is reached (see ref. 1). The frequency of the rotating stall is 1/2 engine speed; this speed relation was unaffected by changes in either altitude or compressor pressure ratio. Rotating stalls generally rotate at about 1/2 engine speed in axial-flow multistage compressors (refs. 3 and 5).

Stage performance. - Equivalent pressure ratios (pressure ratio corrected for speed variations, ref. 8) are calculated for several groups of compressor stages and are shown as a function of corrected engine speed in figure 9. The interstage rakes effectively divided the compressor into four sections as follows: stages 1 to 4, 5 to 7, 8 to 10, and 11 to 12. Equivalent pressure ratios for the early stages indicate the same discontinuities for the different regions of compressor operation that were evident from the preceding curves. Pressure ratios calculated near the blade tips for stages 1 to 4 were lower than the average values for both rotating and tip stall. The stall that occurs at low speed in the early stages forces the blade tips to operate at higher than average pressure ratio or blade loading for stages 5 to 10. For stages 11 to 12, the discontinuities for stalled to stall-free operation are no longer evident, and the pressure ratios are slightly higher for the blade tips.

Stage pressure coefficient  $\psi$  is plotted as a function of flow coefficient  $\phi$  in figure 10, for the same group of points shown in figure 9. Because the flow coefficient varies inversely with angle of attack, these curves are indicative of the range over which the stages operate. As would be expected, the angle-of-attack range for the early stages is relatively large in going from unstalled to tip-stall operation. However, as is typical for axial-flow compressors, some of the compressor midstages (8 to 10) operate over narrow ranges of angle of attack and blade loading (see ref. 8). The outlet stages operate over a wide pressure-coefficient range. At the high flow coefficient (speeds below 5500 rpm and low angle of attack), the outlet stages are turbing, as evidenced by the negative stage pressure coefficient.

Inlet-guide-vane position. - For all the preceding curves, the inlet guide vanes were set in the open or design position. In order to improve the compressor low-speed performance, the inlet guide vanes could be rotated to change the angle of attack.

Tip pressure ratios and efficiencies across the first rotor stage are shown as functions of engine speed in figure 11(a). In the low-speed region where tip stall is present with the inlet guide vanes open, the pressure ratios and efficiencies are relatively low. Increasing speed through the rotating stall and into the stall-free region improves both parameters. Closing the guide vanes at low speeds raises both the pressure ratio and efficiency compared with open-vane operation. At speeds above about 6700 rpm, the blade tips are negatively stalled, as

evidenced by the pressure ratios less than 1.0. The angle of attack with the guide vanes in the closed position is thus considerably reduced from that with the open position. Over-all compressor pressure ratio, corrected air flow, and efficiency are shown as functions of corrected engine speed in figures 11(b), (c), and (d), respectively. Elimination of the stalled operation improves all these parameters in the low-speed region. The improvement in performance with inlet guide vanes closed is especially evident in terms of efficiency; at a speed of 5200 rpm, the efficiency was improved 12 points by closing the guide vanes.

### Compressor Surge Characteristics

In order to determine the compressor surge characteristics, engine accelerations were made over a wide range of operating conditions. During these accelerations, two types of compressor surge were encountered when the inlet guide vanes were in the open position. Typical oscillograph traces taken during acceleration with each type of surge are shown in figure 12. Hot-wire-anemometer traces taken during these surges are presented in figure 13. Because the chart speed for recording the hot-wire-anemometer output was much higher than that of the oscillograph traces in figure 12, a more detailed picture of the flow fluctuations can be seen. The surging shown by the trace in figure 13(a) (corresponding to oscillograph trace in fig. 12(a)) is termed surge with stall, because a single rotating stall is continually superimposed on the surge oscillations. The more violent surge of figure 12(b) has a rotating stall present only a small portion of a given surge cycle, as indicated in figure 13(b).

The frequency and amplitude of the compressor pulsations during surge are presented as functions of engine speed in figure 14. Frequency of surge with stall is slightly higher, and amplitude of surge with stall is considerably lower than that obtained for compressor surge. Increasing speed reduces the frequency of both surge types and increases the amplitude of surge with stall. Engine-speed changes have little effect on the more violent surge amplitude.

In order to provide a more complete physical understanding of succeeding figures, examples of types of surge encountered during engine accelerations are shown by time histories of compressor pressure ratio as a function of corrected engine speed in figures 15 and 16 for inlet guide vanes open and closed, respectively. The acceleration shown in figure 15(a) started from the tip-stall region of compressor operation. Immediately following the initial fuel increase, there was a partial quenching effect and then a rise in pressure ratio to point A, which is the greatest distance above steady-state operation. The pressure ratio then increases along with engine speed to 6020 rpm (point B), where the compressor goes into surge. The pressure ratio at this point

has deteriorated to below the steady-state operating line. These oscillations encountered during accelerations from the steady-state stall regions invariably have rotating-stall pulsations superimposed on the surge cycles and are thus termed surge with stall. The loci of maximum pressure-ratio points during the oscillations define the line of limiting pressure ratio for surge with stall; minimum pressure-ratio points define the surge-with-stall recovery line. The final recovery (point C) occurred in the higher-speed portion of the rotating-stall region. In this region, operation is close to stall-free conditions, as is shown by the first-stage pressure-coefficient curve in figure 10.

An acceleration from the upper branch of the steady-state operating line in the hysteresis area (approximately 6200 to 6500 rpm in figs. 11(b) to (d)) is shown in figure 15(b) where the compressor surges at a pressure ratio of 4.0 at 5900 rpm. It should be remembered that, although the compressor is operating stall-free before acceleration, it is in the speed region where rotating stall exists following a speed increase. The stall-free operation at this point arises from a speed reduction from the high-speed stall-free operation and the hysteresis phenomenon previously discussed. After the initial surge oscillation, the compressor goes into surge with stall, from which the final recovery was obtained at a corrected speed of 6100 rpm. This sequence is characteristic when the surge is obtained in the range of speeds where rotating stall can exist in the steady-state condition.

A similar acceleration from the stall-free operating region but at a speed above the rotating-stall region is shown in figure 15(c). Surge is encountered at 6620 rpm; complete recovery is then obtained at 6680 rpm. When fuel steps much larger than that which caused the surge in figure 15(c) were injected into the engine, combustor blow-out sometimes occurred during the initial surge cycle. A successful acceleration such as that shown in figure 15(d) resulted when the fuel step was smaller than that used for the acceleration in figure 15(c).

When the inlet guide vanes were in the closed position, a single type of surge was obtained. Neither tip stall nor rotating stall was encountered during steady-state closed-guide-vane operation or engine acceleration. An acceleration with a fuel step large enough to produce surge is presented in figure 16.

Compressor surge maps. - By collecting the compressor surge and recovery points from many accelerations, it is possible to define the operational boundaries in terms of compressor pressure ratio and corrected engine speed. For clarity, the surge and recovery limits obtained from accelerations from the stall region are considered first (fig. 17). Maximum surge-free pressure ratio is indicated by the line slightly above the steady-state operating lines with stall. This line represents the loci of points such as A on figure 15(a), as well as

similar points from successful accelerations through this region. Larger fuel steps ultimately resulted in surge with stall, although the pressure oscillations generally did not occur until the pressure ratio deteriorated to a point slightly below the steady-state operating line (see point B, fig. 15(a)). The speed at which the oscillation commences is determined by the size of the fuel step; that is, for the acceleration shown in figure 15(a), a larger fuel step would not have resulted in higher pressure ratios, but rather a lower speed for the first surge cycle. As shown in figure 15(a), during surge with stall the pressure ratio oscillated between the surge-with-stall line and the recovery line shown in figure 17. The speed at which the surge with stall ceased (point C, fig. 15(a)) was unpredictable but varied between about 6200 and 7000 rpm.

The surge limits obtained with guide vanes open for accelerations from stall-free steady-state operation are shown in figure 18. Compressor surge and recovery points define respective single lines for variations in flight Mach number, altitude, and inlet-air temperature, as shown in figures 18(a), (b) and (c), respectively. It should be remembered that the compressor will oscillate between the surge pressure ratio and recovery lines shown in figure 18 only if the engine speed is above that at which rotating stalls normally exist. If the speed is in the region where rotating stalls can exist, the first surge cycle will be followed by less severe oscillations between the surge-with-stall line and the recovery line (see acceleration in fig. 15(b)).

Similar curves are given in figure 19 for the inlet guide vanes in the closed position. There was little or no effect of Mach number, altitude, or inlet-air temperature on the surge or surge recovery lines. Closing the inlet guide vanes moved the surge recovery line to a position above the steady-state operating line.

A direct comparison of the effect of inlet-guide-vane position on the surge (or acceleration) margin is shown in figure 20, where the surge pressure ratio is divided by steady-state pressure ratio and plotted as a function of engine speed. This ratio is a measure of the pressure-ratio margin available for acceleration. With the guide vanes open, the margin is relatively low in the tip-stall region and is almost negligible in the rotating-stall region. Increasing speed, which eliminates the compressor stall, results in a large improvement in acceleration margin. Moving the guide vanes to the closed position resulted in a large improvement in the acceleration over the entire range of engine speeds. The most striking effect of closing the inlet guide vanes is in the low-speed region. At 5400 rpm there is a 9.5-percent margin between surging and steady-state operation in tip stall with inlet guide vanes open; closing the vanes increases the margin to 19.5 percent. At 6200 rpm the increase was from 1.5 to 30 percent. Thus, closing the inlet guide vanes, which eliminated the stall, resulted in

a two- to twentyfold increase in the acceleration margin. The desirability of varying the inlet guide vanes on this compressor is quite evident.

Surge fuel flows. - To aid in the design of engine control systems incorporating surge protection, the surge limits are correlated in terms of engine fuel flow and engine speed. The method of establishing the engine fuel-flow limit for compressor surge is demonstrated in figure 21. At a given engine speed, sufficient fuel steps were made to determine the lowest fuel flow that would result in compressor surge, or surge followed by blow-out. These data points established a boundary such as that shown in figure 21. The line then represents the highest fuel flow that can be put into the engine and still produce a surge-free acceleration. The time to increase the fuel flow a given amount was varied from 0.02 to 2.0 seconds; however, the rate of fuel input did not affect the location of the surge line.

The effect of flight condition on the fuel-flow surge lines is shown for the inlet guide vanes in the open and closed positions, respectively, in figures 22 and 23. Because the guide vanes are engine-speed scheduled to open in the vicinity of 6800 rpm, surge fuel flows were not obtained in the low-speed region with the inlet guide vanes open. In general, decreasing flight Mach number or inlet Reynolds number (increasing altitude) reduced the fuel flow required for compressor surge; whereas, smaller effects were evident on the pressure ratio for surge. This may be a Reynolds number effect on the compressor characteristic lines in the vicinity of surge. Because the characteristic line probably has little slope at the surge condition (see ref. 9), Reynolds number effects would not be as apparent in terms of pressure ratio as in engine fuel flow.

The effect of inlet-guide-vane position on fuel-flow acceleration margin is shown in figure 24. The acceleration margin is represented by the surge fuel flow divided by the steady-state fuel flow. Closing the inlet guide vanes markedly improves the acceleration fuel-flow margin as well as the pressure-ratio margin (fig. 20).

Surge reproducibility. - The qualitative effects shown by the preceding curves are believed to be general for the engine investigated. However, engine reproducibility has a large effect on some of the quantitative measurements obtained. For instance, the pressure ratios and surge fuel flows obtained for the four engines used in the investigation (two engines, each rebuilt once) are presented in figure 25. During rebuilding, no aerodynamic changes were made; however, the engines were completely disassembled to check all the mechanical parts. Although both the steady-state compressor pressure ratios and engine fuel flows agree reasonably well, there are considerable differences in the surge pressure ratios and fuel flows. At 7600 rpm, the surge pressure ratios

differ by as much as 6 percent; the fuel flows at surge differ as much as 32 percent. These differences indicate the importance of obtaining the lowest compressor surge and engine fuel-flow limits that may be reasonably expected, for the purpose of determining a generally applicable engine control fuel schedule.

#### SUMMARY OF RESULTS

A turbojet engine with variable inlet guide vanes was investigated in an altitude test facility to determine the steady-state compressor performance and surge characteristics. When the compressor was operated with the inlet guide vanes in the open (design) position, three distinct regions of compressor operation were obtained: low speed where the blade tips in the early stages were stalled, medium speed where one rotating stall existed, and high speed where the compressor operated stall-free. Closing the inlet guide vanes eliminated the stalled regions and considerably improved the compressor performance in terms of air flow, pressure ratio, and efficiency in the low-speed region. Closing the vanes also eliminated the steady-state stalled region and improved the acceleration margin two- to twentyfold.

Compressor surge pressure ratios were unaffected by changes in flight condition for either position of the inlet guide vanes. However, decreasing the inlet Reynolds number reduced the corrected fuel flow required for compressor surge. Reproducibility of the experimental data obtained from several engines had a small effect on the surge pressure ratio, but a sizable effect on the fuel flow required for surge.

Lewis Flight Propulsion Laboratory  
National Advisory Committee for Aeronautics  
Cleveland, Ohio, October 4, 1954.

3494

CZ-2 back

## APPENDIX - SYMBOLS

The following symbols are used in this report:

$c_p$	specific heat at constant pressure
$g$	acceleration due to gravity, 32.2 ft/sec <sup>2</sup>
$J$	mechanical equivalent of heat, 778.2 ft-lb/Btu
$N$	engine speed, rpm
$P$	total pressure, lb/sq ft abs

$$\left(\frac{P_1}{P_0}\right)_e \quad \text{equivalent pressure ratio,} \quad \left[ \frac{\left(\frac{\Delta T}{T_1}\right)_{ad} \left(\frac{U_1}{\sqrt{T_1}}\right)_d^2}{\left(\frac{U_1}{\sqrt{T_1}}\right)^2} + 1 \right]^{\frac{\gamma}{\gamma-1}}$$

$T$	total temperature, °F abs
$U$	mean blade speed, ft/sec
$V$	velocity, ft/sec
$W$	air flow, lb/sec
$W_f$	fuel flow, lb/hr
$\gamma$	ratio of specific heats
$\delta$	pressure-correction factor, ratio of total pressure to NACA standard sea-level pressure, P/2116
$\eta$	compressor efficiency
$\theta$	temperature-correction factor, ratio of total temperature to NACA standard sea-level temperature, T/518.7
$\rho$	density, slugs/cu ft
$\phi$	flow coefficient, $V_a/U$

$$\psi = \frac{gJc_p T_i \left[ \left( \frac{P_o}{P_i} \right)^{\frac{\gamma-1}{\gamma}} - 1 \right]}{U^2}$$

pressure coefficient,

Subscripts:

a	axial
ad	adiabatic
av	average
d	design
e	equivalent
h	hub
i	stage inlet
l	local
o	stage outlet
t	tip
1	engine inlet
2	compressor inlet
2a	first stator stage
2b	fourth stator stage
2c	seventh stator stage
2d	tenth stator stage
3	compressor outlet

#### REFERENCES

1. Benser, William A.: Analysis of Part-Speed Operation for High-Pressure-Ratio Multistage Axial-Flow Compressors. NACA RM E53I15, 1953.

2. Huppert, Merle C.: Preliminary Investigation of Flow Fluctuations During Surge and Blade Row Stall in Axial-Flow Compressors. NACA RM E52F28, 1952.
3. Huppert, Merle C., Costilow, Eleanor L., and Budinger, Ray E.: Investigation of a 10-Stage Subsonic Axial-Flow Research Compressor. III - Investigation of Rotating Stall, Blade Vibration, and Surge at Low and Intermediate Compressor Speeds. NACA RM E53C19, 1953.
4. Iura, T., and Rannie, W. D.: Observations of Propagating Stall in Axial-Flow Compressors. Rep. No. 4, Mech. Eng. Lab., C.I.T., Apr. 1953. (Navy Contract N6-ORI-102, Task Order 4.)
5. Huppert, Merle C., Johnson, Donald F., and Costilow, Eleanor L.: Preliminary Investigation of Compressor Blade Vibration Excited by Rotating Stall. NACA RM E52J15, 1952.
6. Huppert, Merle C., Calvert, Howard F., and Meyer, André J.: Experimental Investigation of Rotating Stall and Blade Vibration in the Axial-Flow Compressor of a Turbojet Engine. NACA RM E54A08, 1954.
7. Huntley, S. C., Huppert, Merle C., and Calvert, Howard F.: Effect of Inlet-Air Baffles on Rotating-Stall and Stress Characteristics of an Axial-Flow Compressor in a Turbojet Engine. NACA RM E54G09, 1954.
8. Medeiros, Arthur A., Benser, William A., and Hatch, James E.: Analysis of Off-Design Performance of a 16-Stage Axial-Flow Compressor with Various Blade Modifications. NACA RM E52L03, 1953.
9. Bullock, Robert O., Wilcox, Ward W., and Moses, Jason J.: Experimental and Theoretical Studies of Surging in Continuous-Flow Compressors. NACA Rep. 861, 1946. (Supersedes NACA TN 1213.)

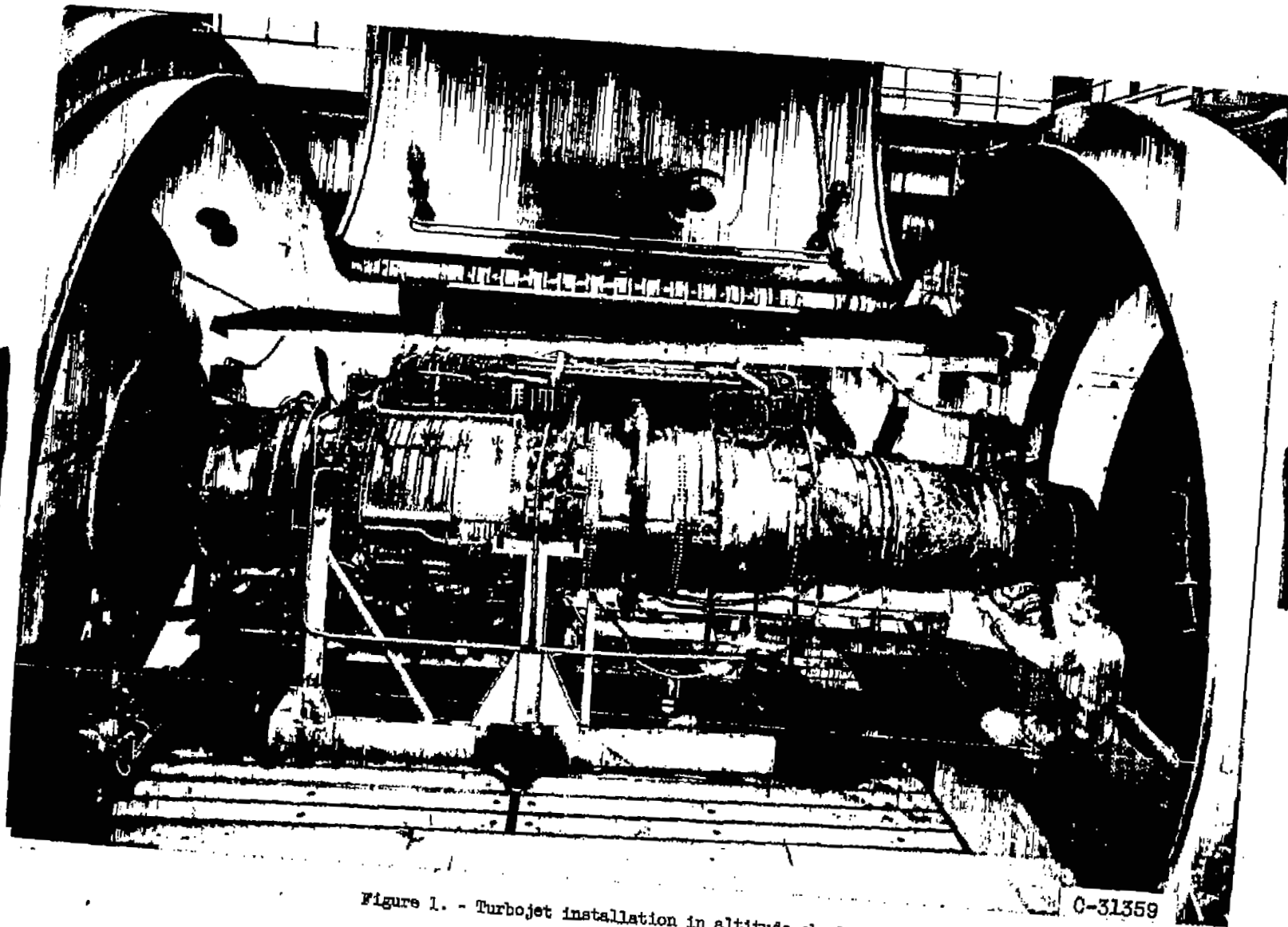


Figure 1. - Turbojet installation in altitude chamber.

C-31359

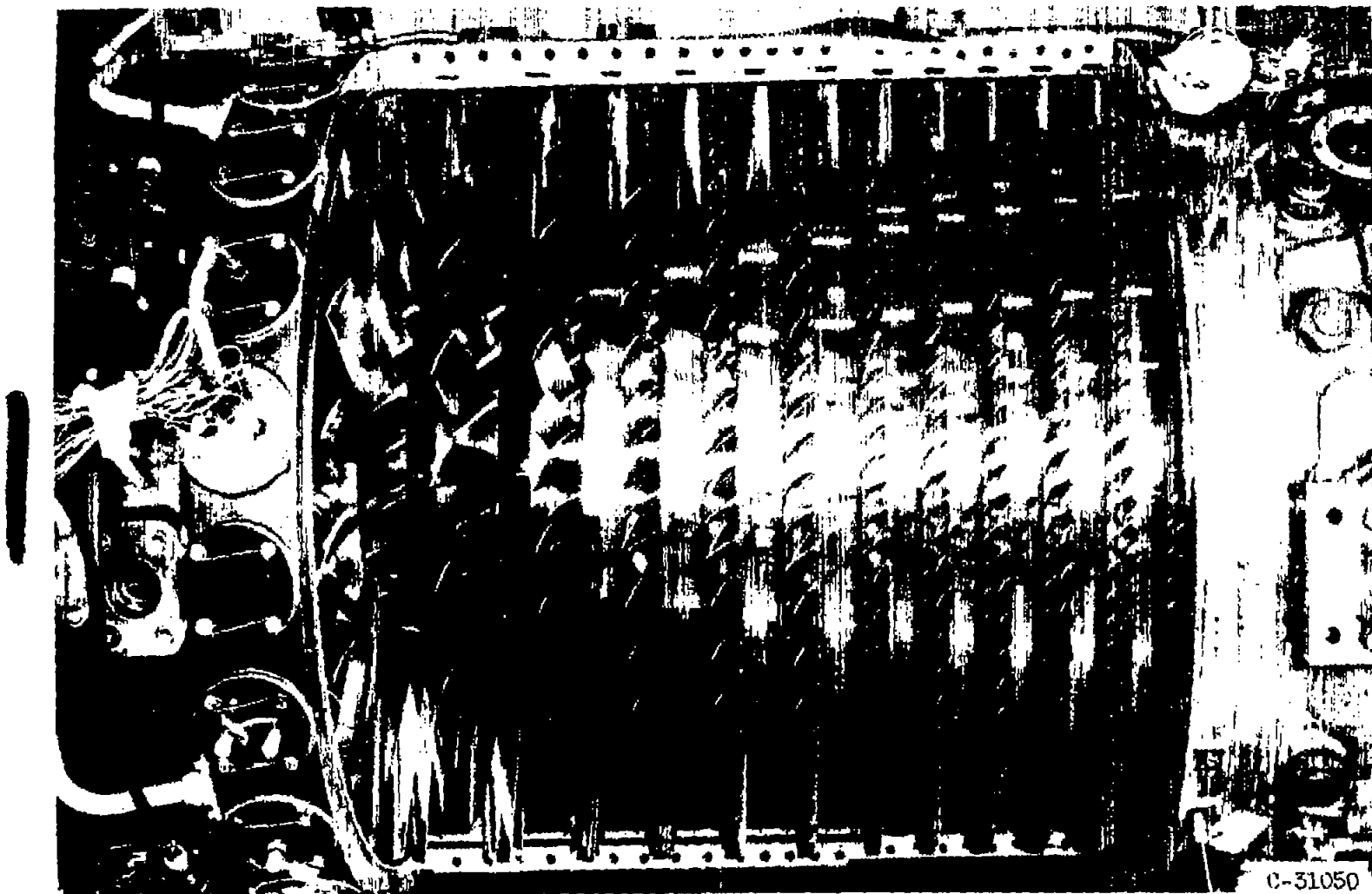
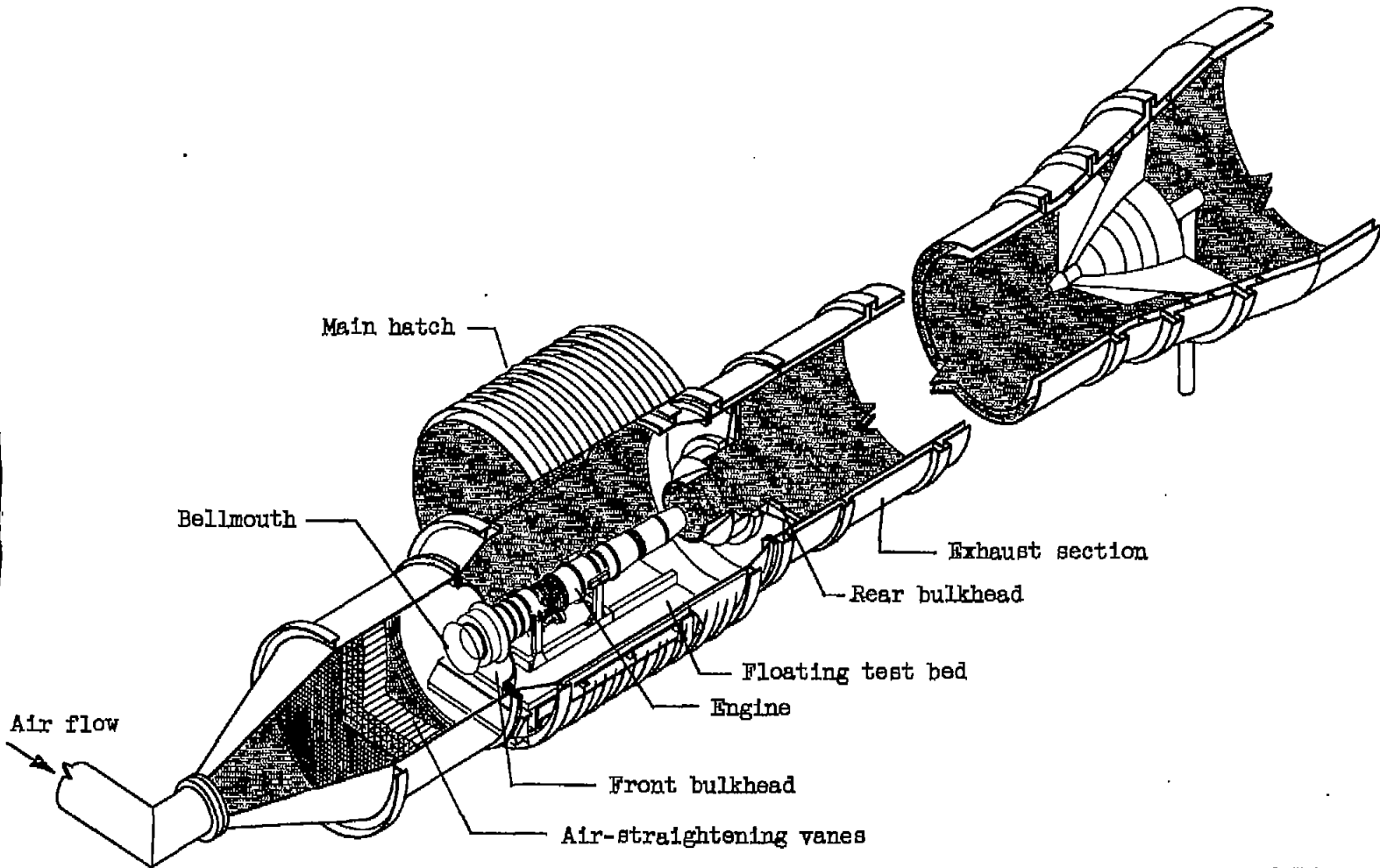
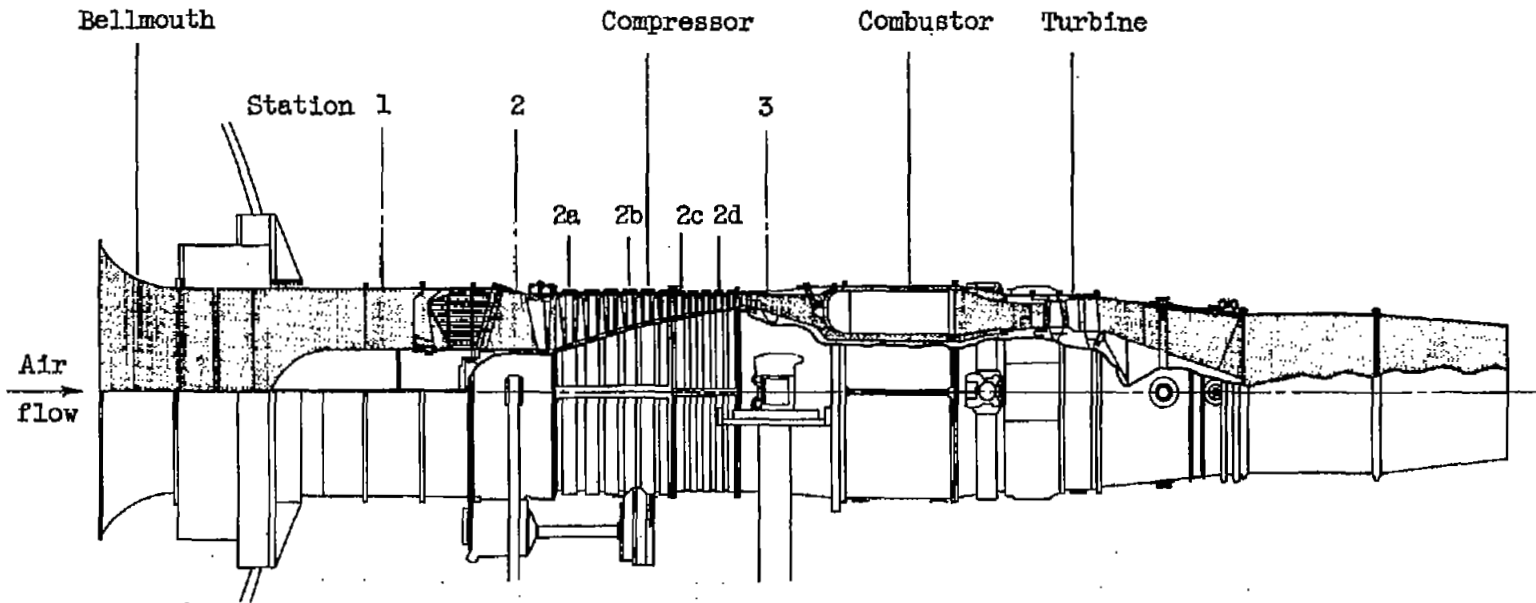


Figure 2. - Compressor rotor.



CD-3237

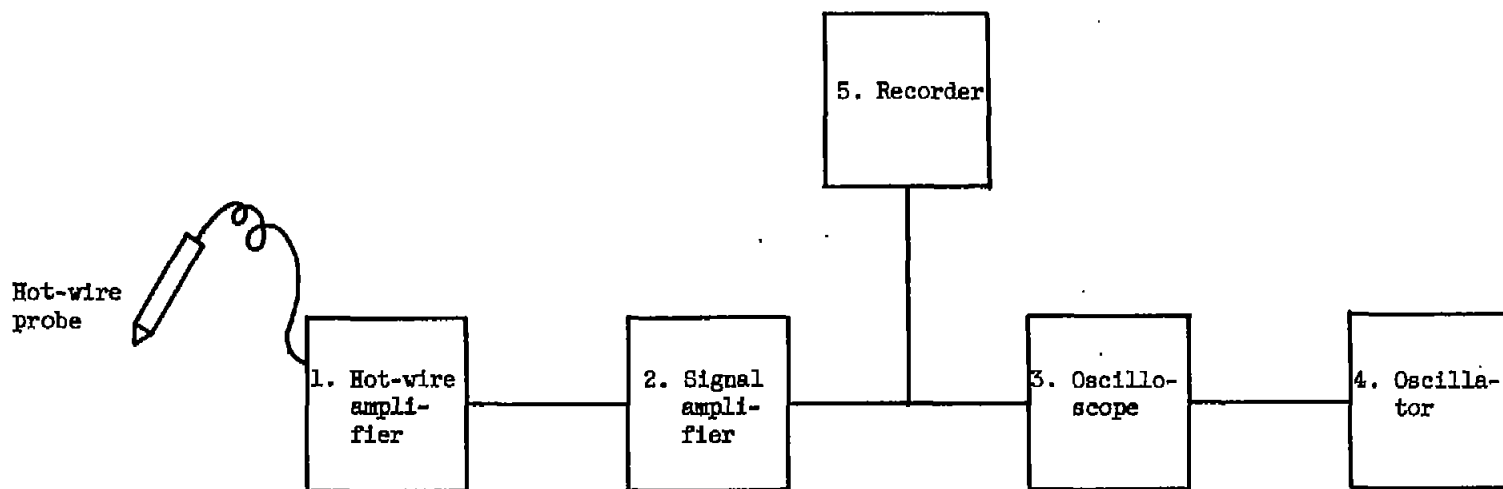
Figure 3. - Schematic sketch of turbojet engine installed in altitude test facility.



Station	Location	Total-pressure tubes	Static-pressure tubes	Wall static-pressure orifices	Thermo-couples
1	Engine inlet	36	16	4	16
2	Compressor inlet	9	2	1	0
2a	First stator	5	0	0	5
2b	Fourth stator	5	0	0	5
2c	Seventh stator	5	0	0	5
2d	Tenth stator	5	0	0	5
3	Compressor outlet	20	4	5	6

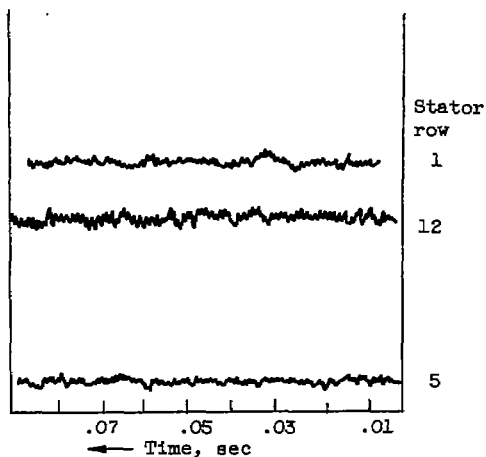
CD-3088

Figure 4. - Cross section of turbojet engine showing instrumentation stations.

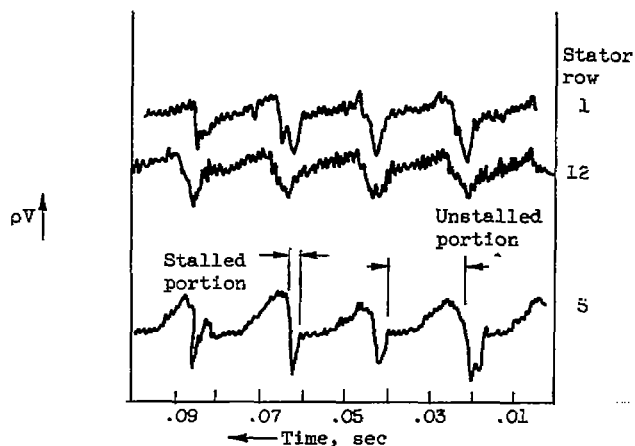


1. Essentially a self-balancing bridge, one arm of which is the wire in the anemometer probe. Supplies sufficient current to maintain hot-wire probe at constant temperature.
2. Controls magnitude of signal output.
3. Visual means of observing  $\mu V$  fluctuations.
4. Means of determining frequency of observed oscillations.
5. Photographic recording of hot-wire signals (max. rate, 48 in./sec).

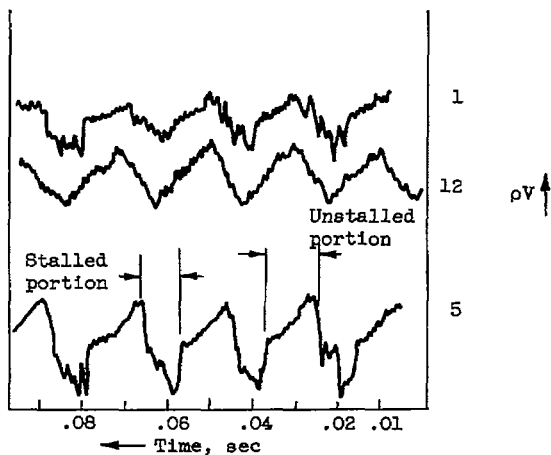
Figure 5. - Schematic of hot-wire-anemometer instrumentation.



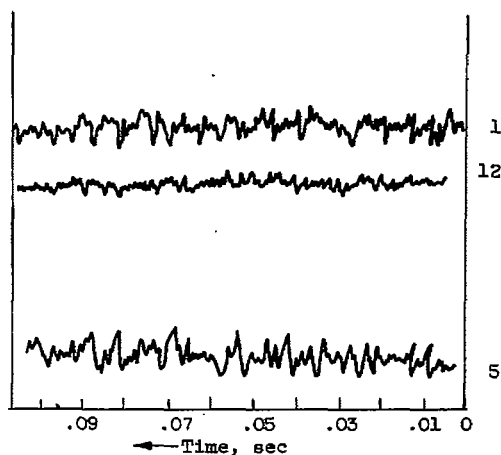
(a) Stall-free operation (speeds above about 6000 rpm).



(b) Rotating stall. High intermediate speed (about 6400 rpm).



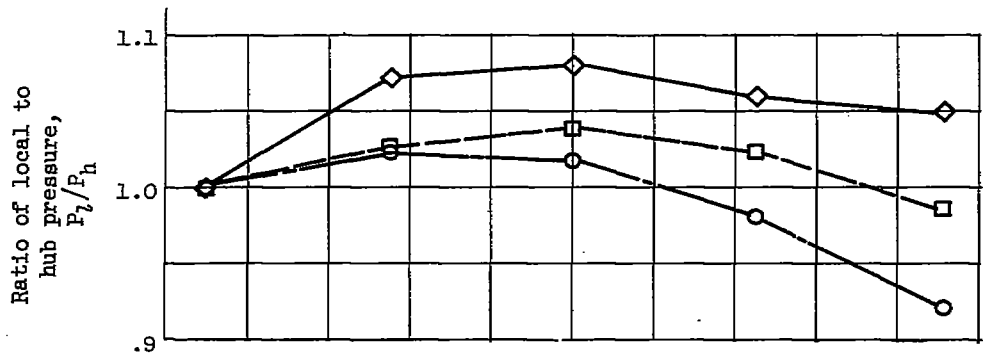
(c) Rotating stall. Low intermediate speed (about 5800 rpm).



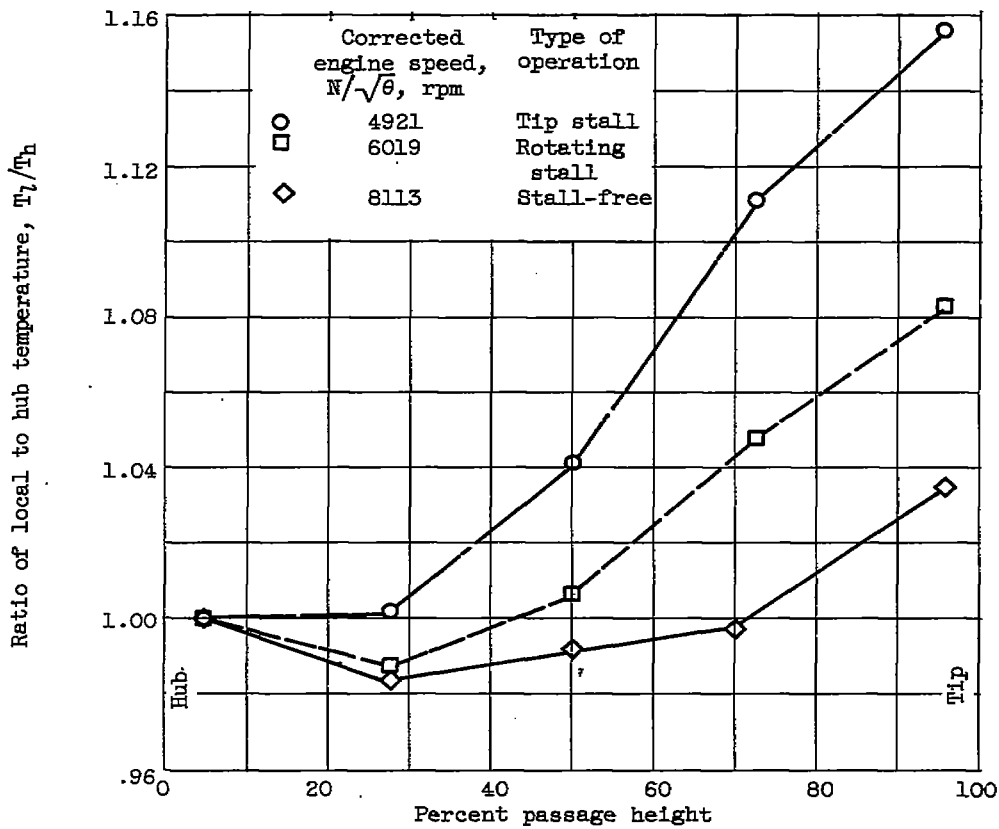
(d) Tip stall region (speeds below 5800 rpm).

Figure 6. - Hot-wire-anemometer traces obtained for various types of steady-state compressor operation. Inlet guide vanes open.

3494

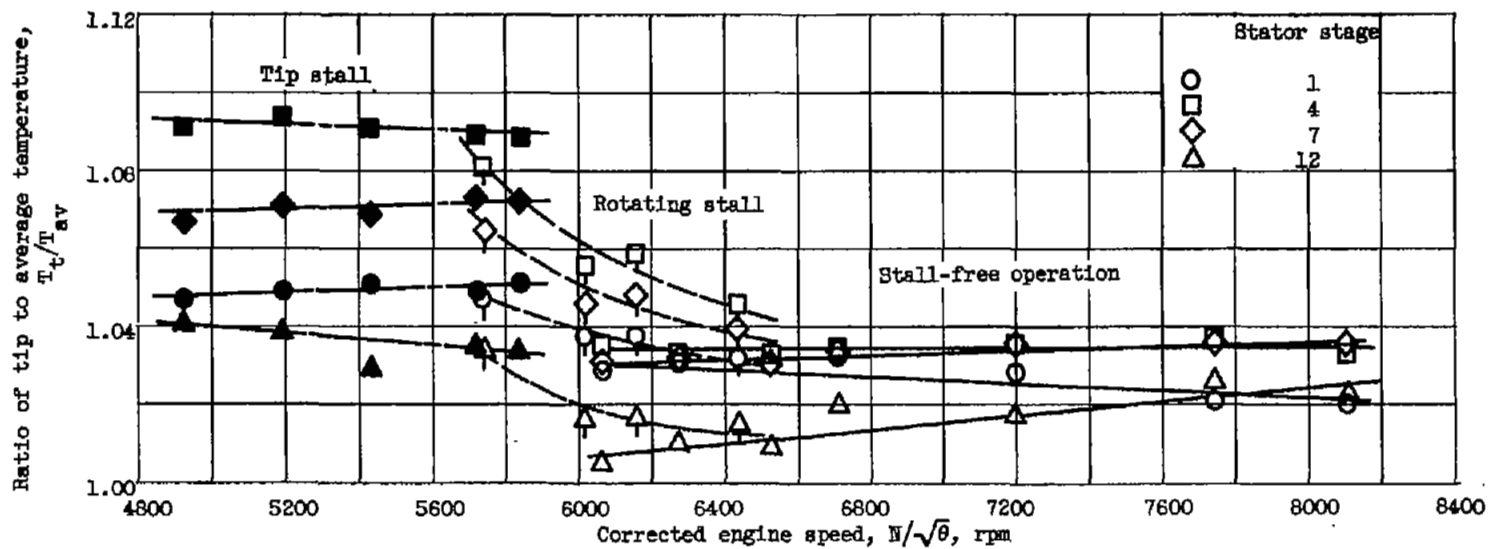


(a) Pressure ratio.



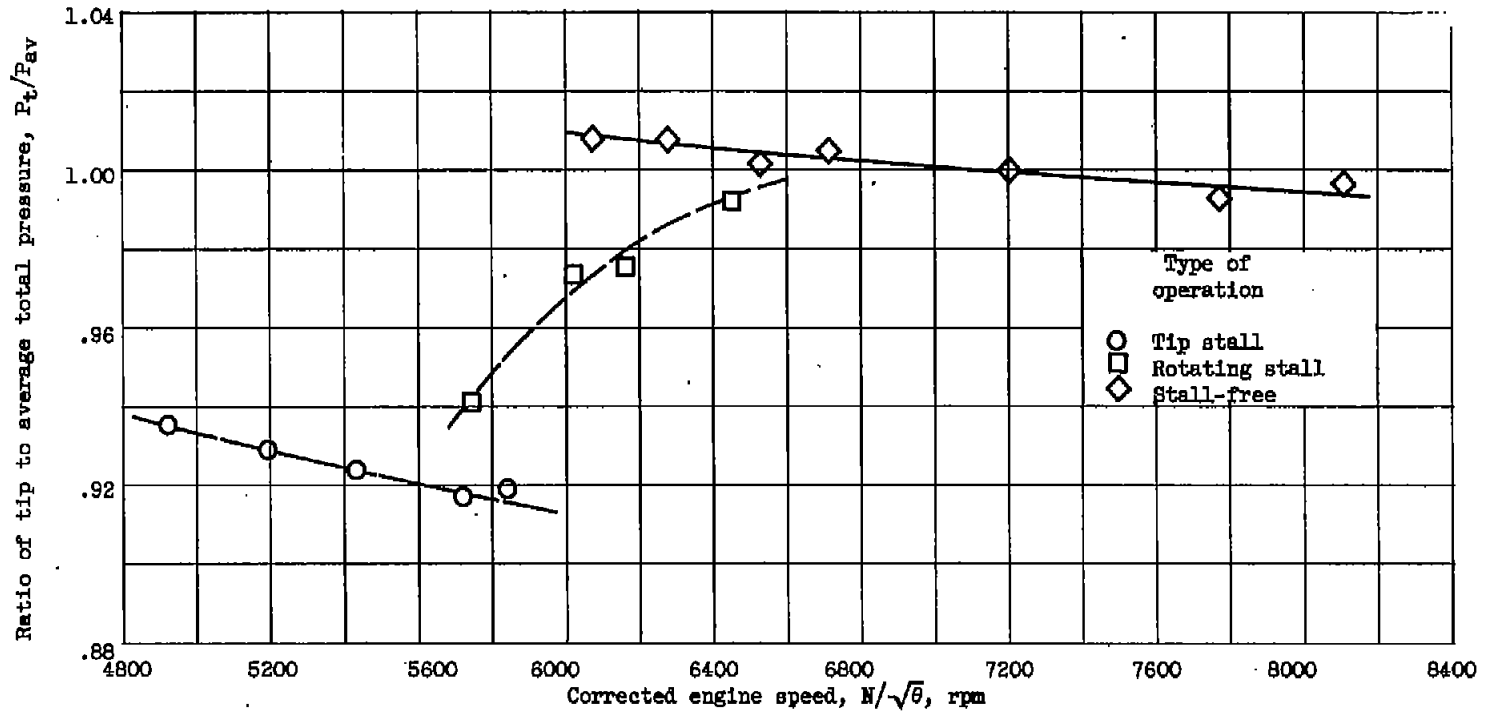
(b) Temperature ratio.

Figure 7. - Variation of interstage pressure and temperature ratios with passage height for three types of compressor operation. Fourth stator stage; inlet guide vanes open.



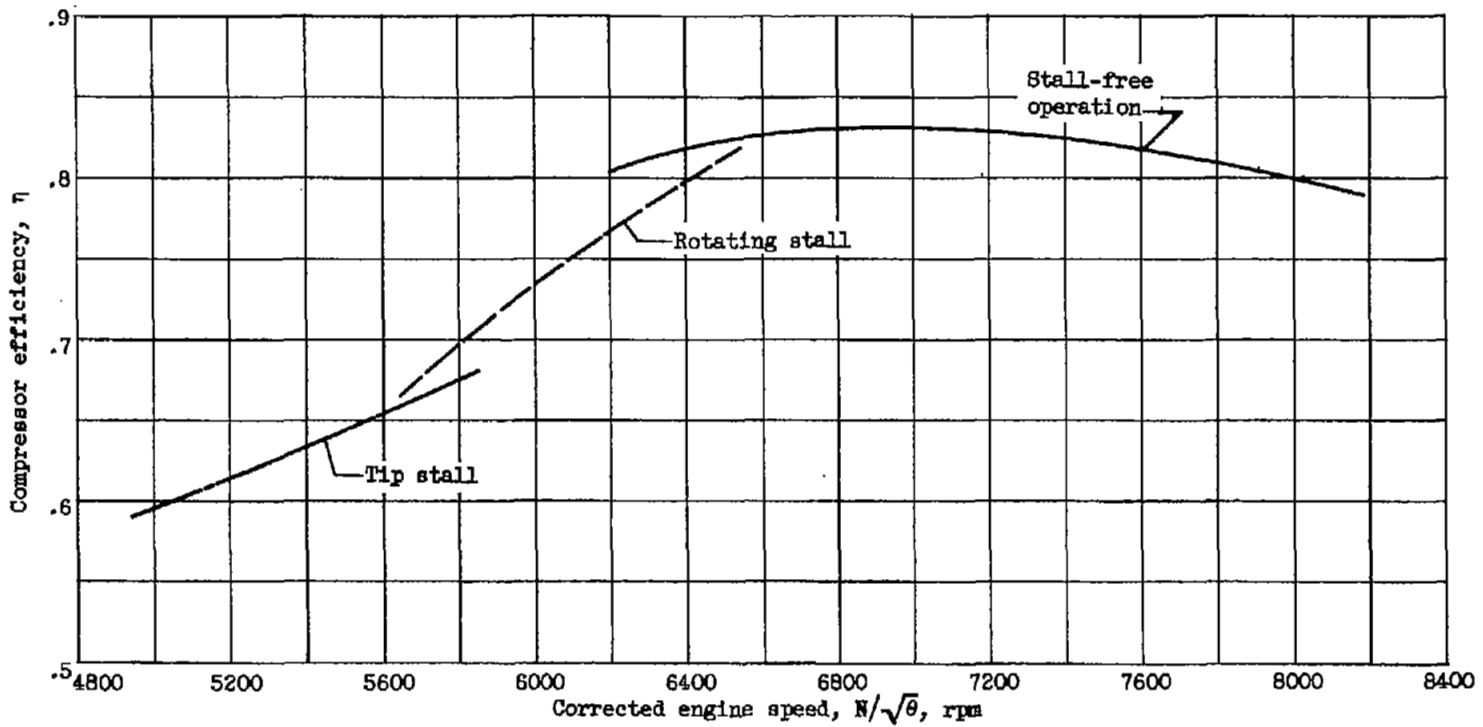
(a) Interstage temperature ratios.

Figure 8. - Variation of performance parameters with corrected engine speed for three types of compressor operation. Inlet guide vanes open.



(b) Interstage pressure ratios. Fourth stator stage.

Figure 8. - Continued. Variation of performance parameters with corrected engine speed for three types of compressor operation. Inlet guide vanes open.



(c) Compressor efficiency.

Figure 8. - Concluded. Variation of performance parameters with corrected engine speed for three types of compressor operation. Inlet guide vanes open.

7675  
CZ-4

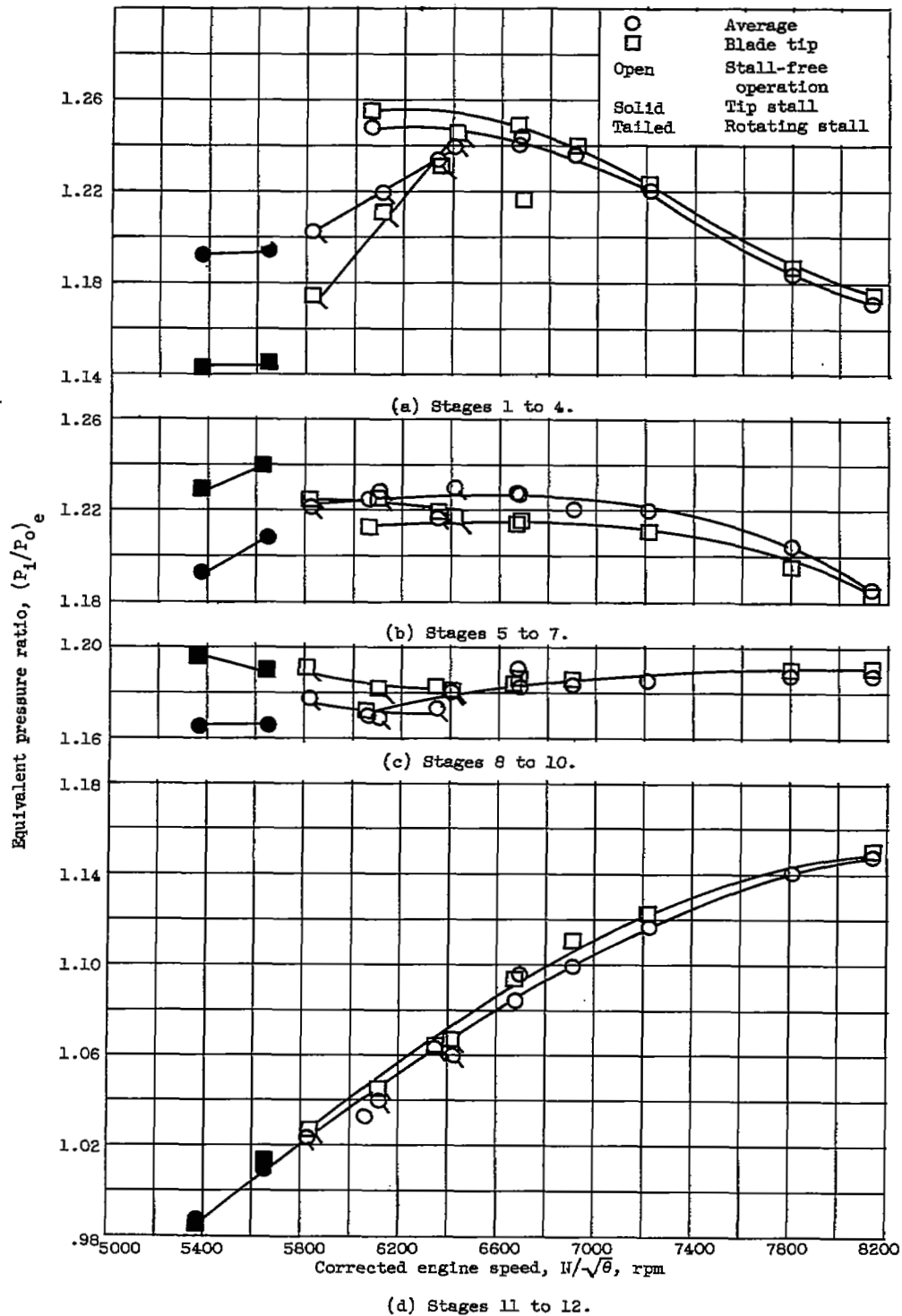


Figure 9. - Variation of equivalent pressure ratio with corrected engine speed for several groups of compressor stages. Inlet guide vanes open.

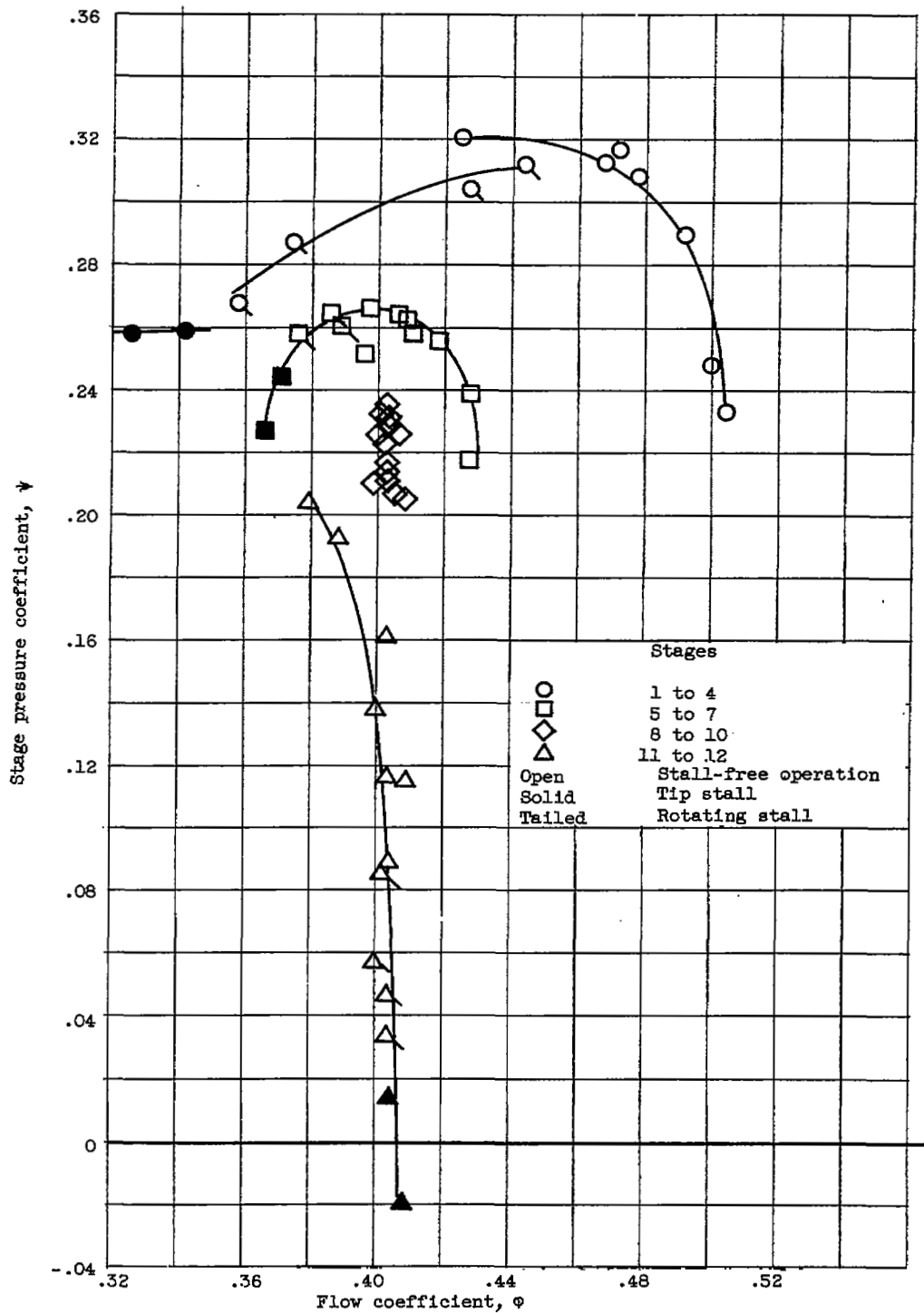
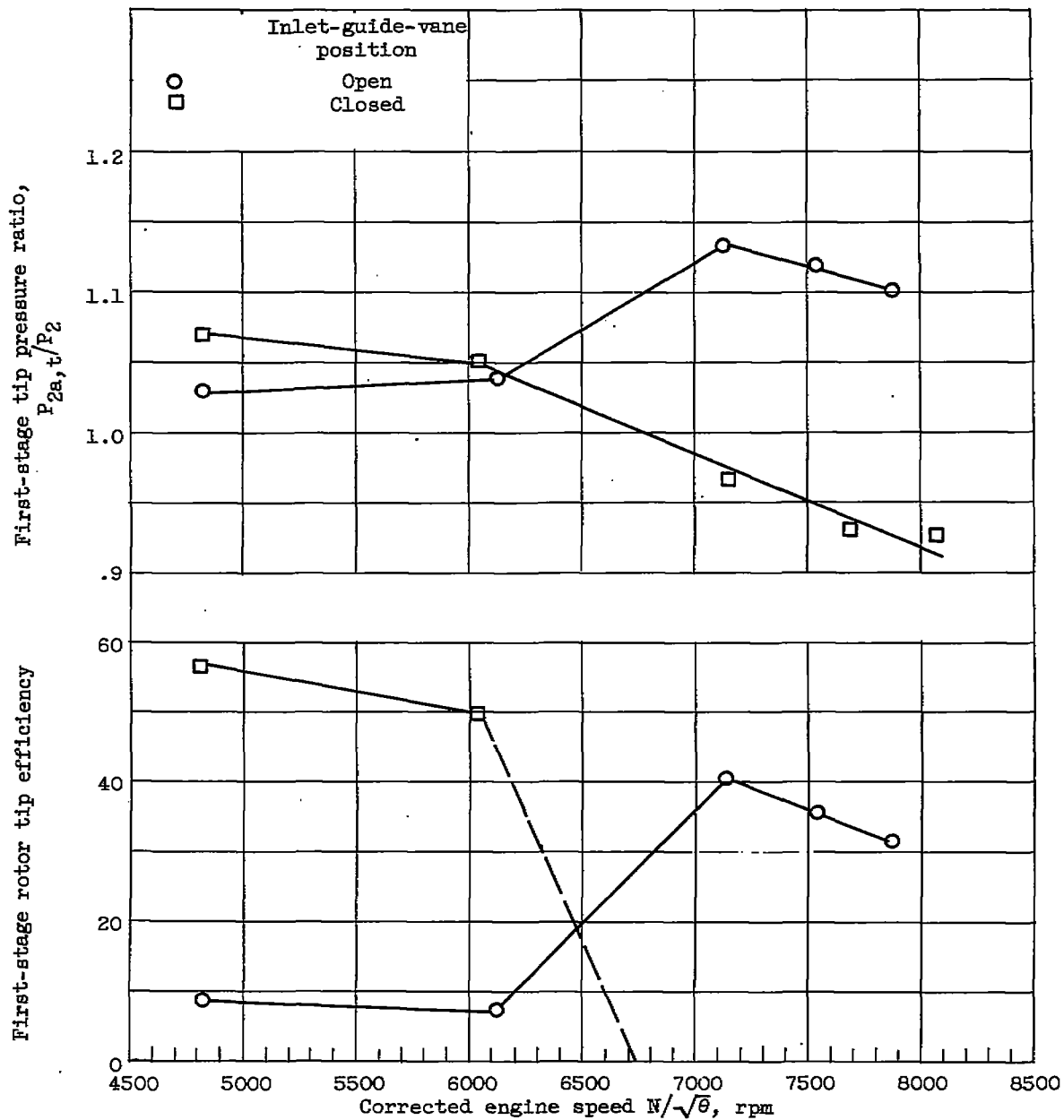


Figure 10. - Variation of stage pressure coefficient with flow coefficient for several groups of compressor stages. Inlet guide vanes open.

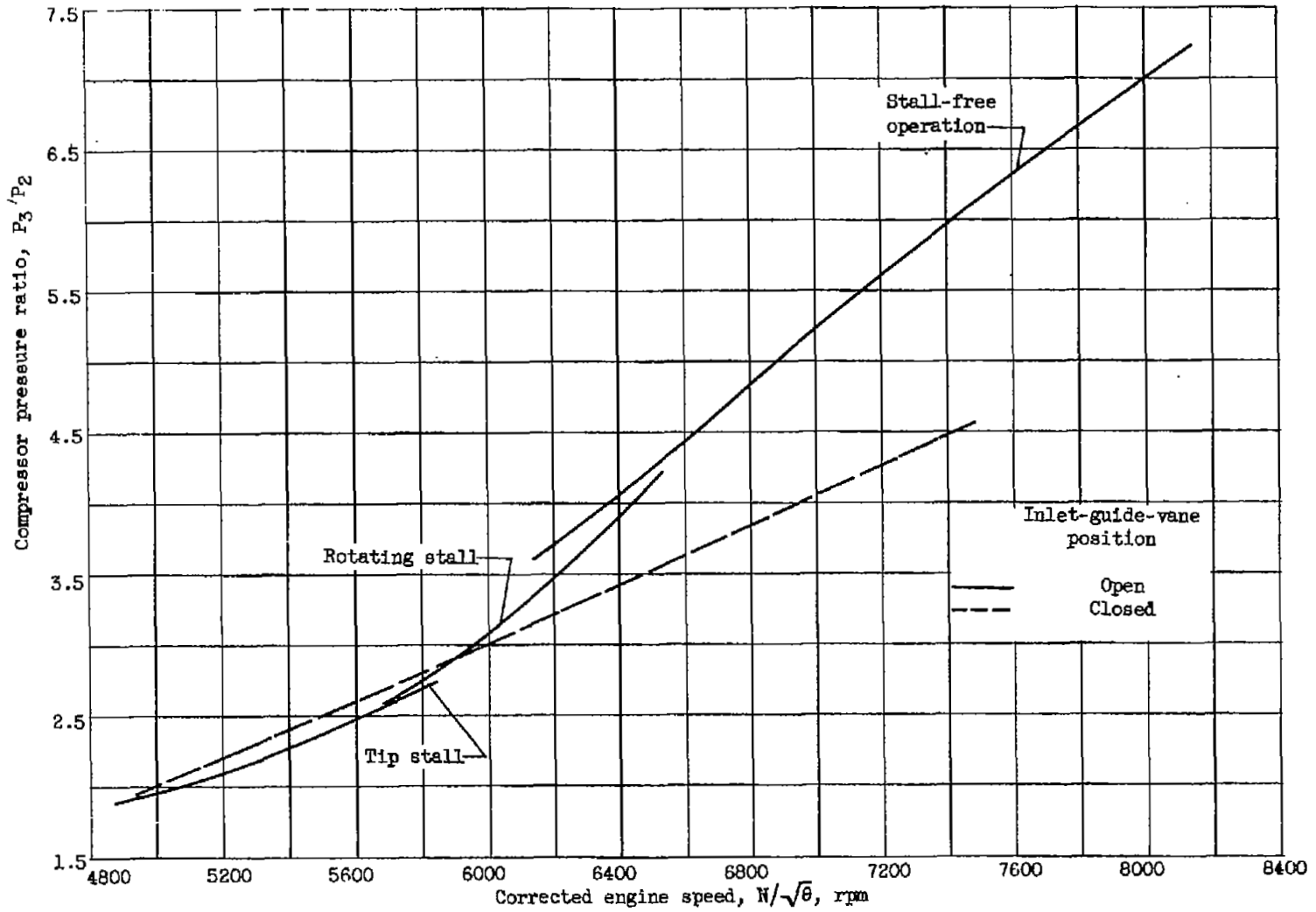
3494

CZ-4 back



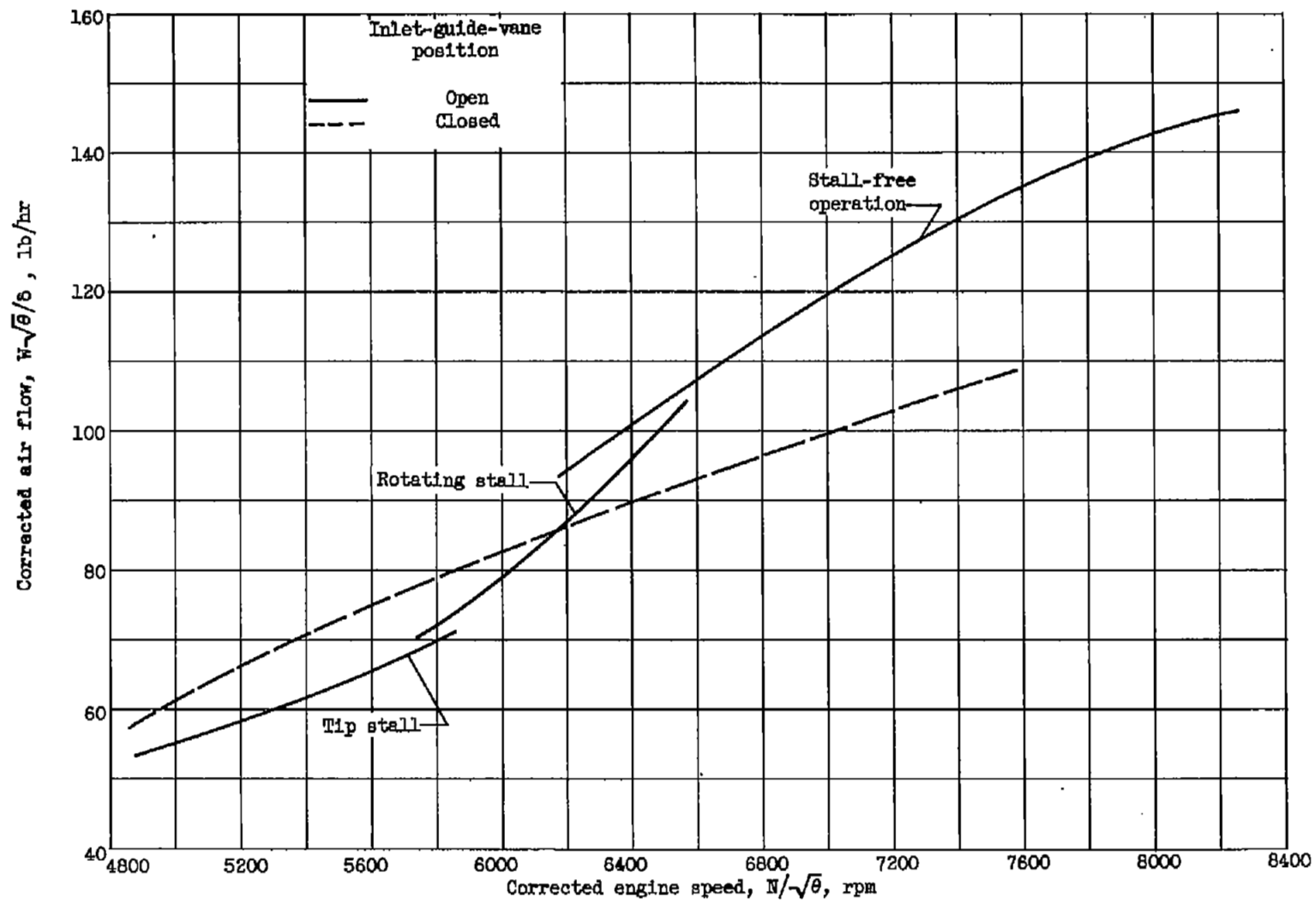
(a) Pressure ratio and efficiency across tip of first rotor stage.

Figure 11. - Effect of inlet-guide-vane position on compressor operation.



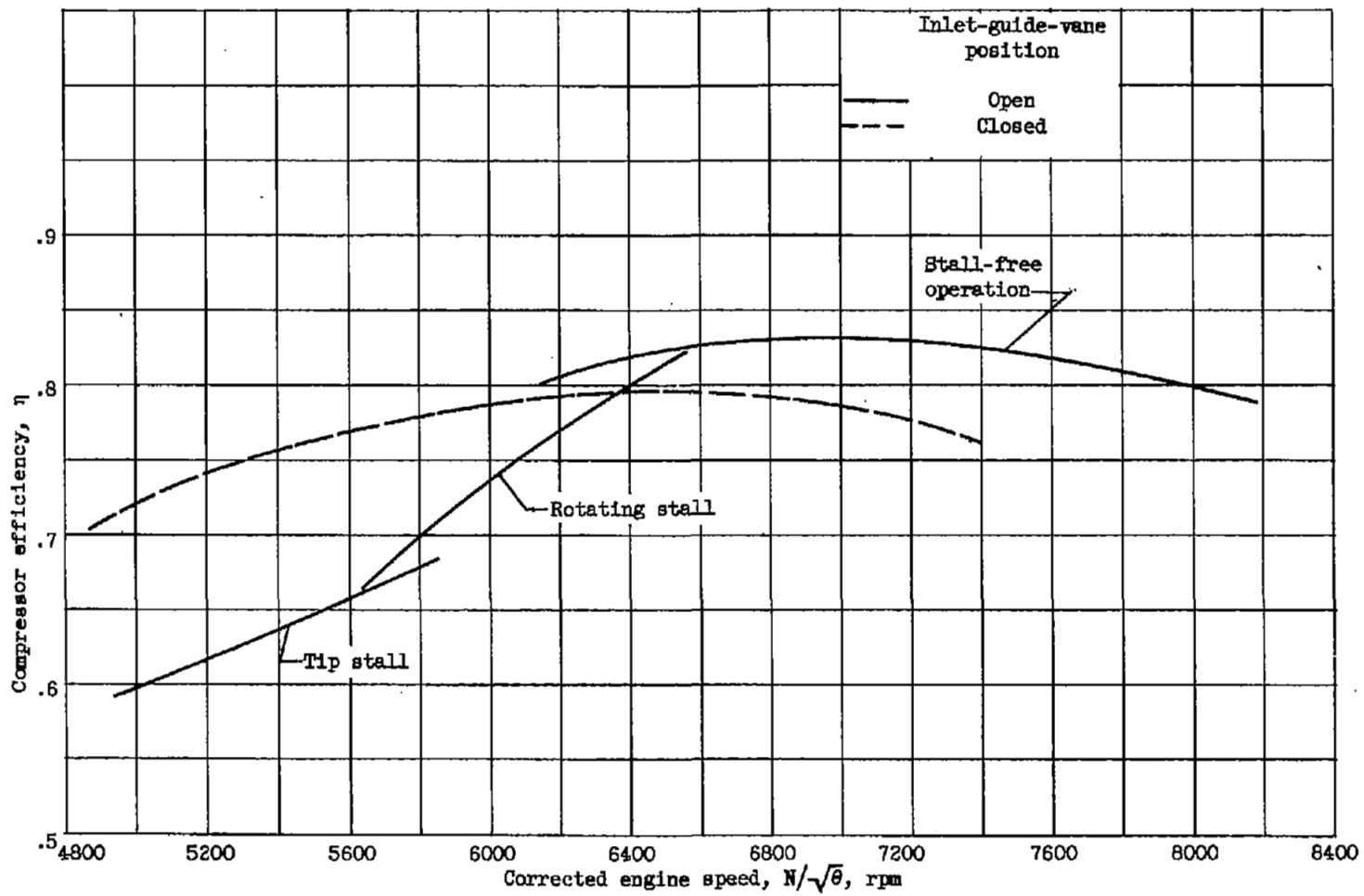
(b) Over-all compressor pressure ratio.

Figure 11. - Continued. Effect of inlet-guide-vane position on compressor operation.



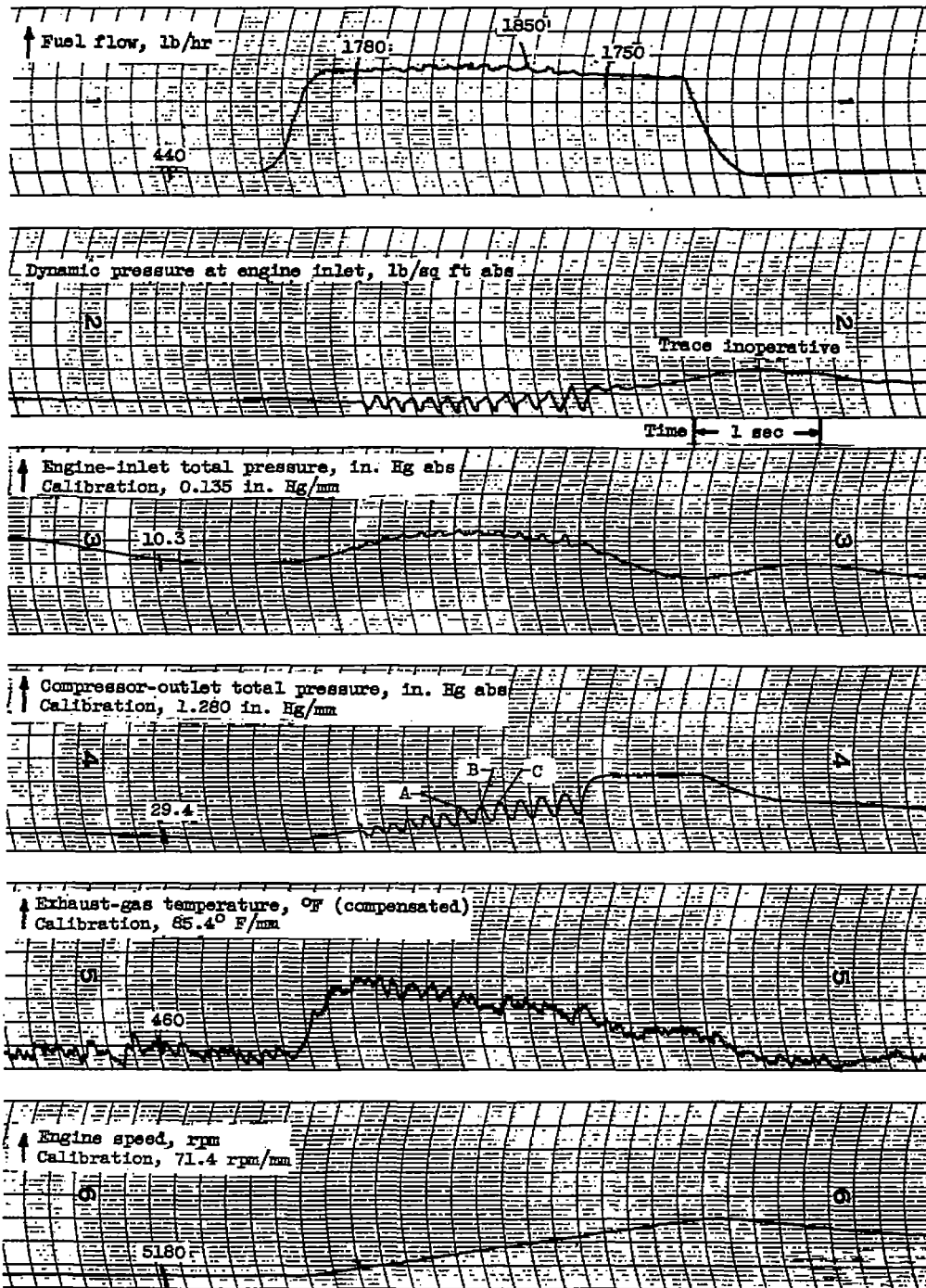
(c) Corrected air flow.

Figure 11. - Continued. Effect of inlet-guide-vane position on compressor operation.



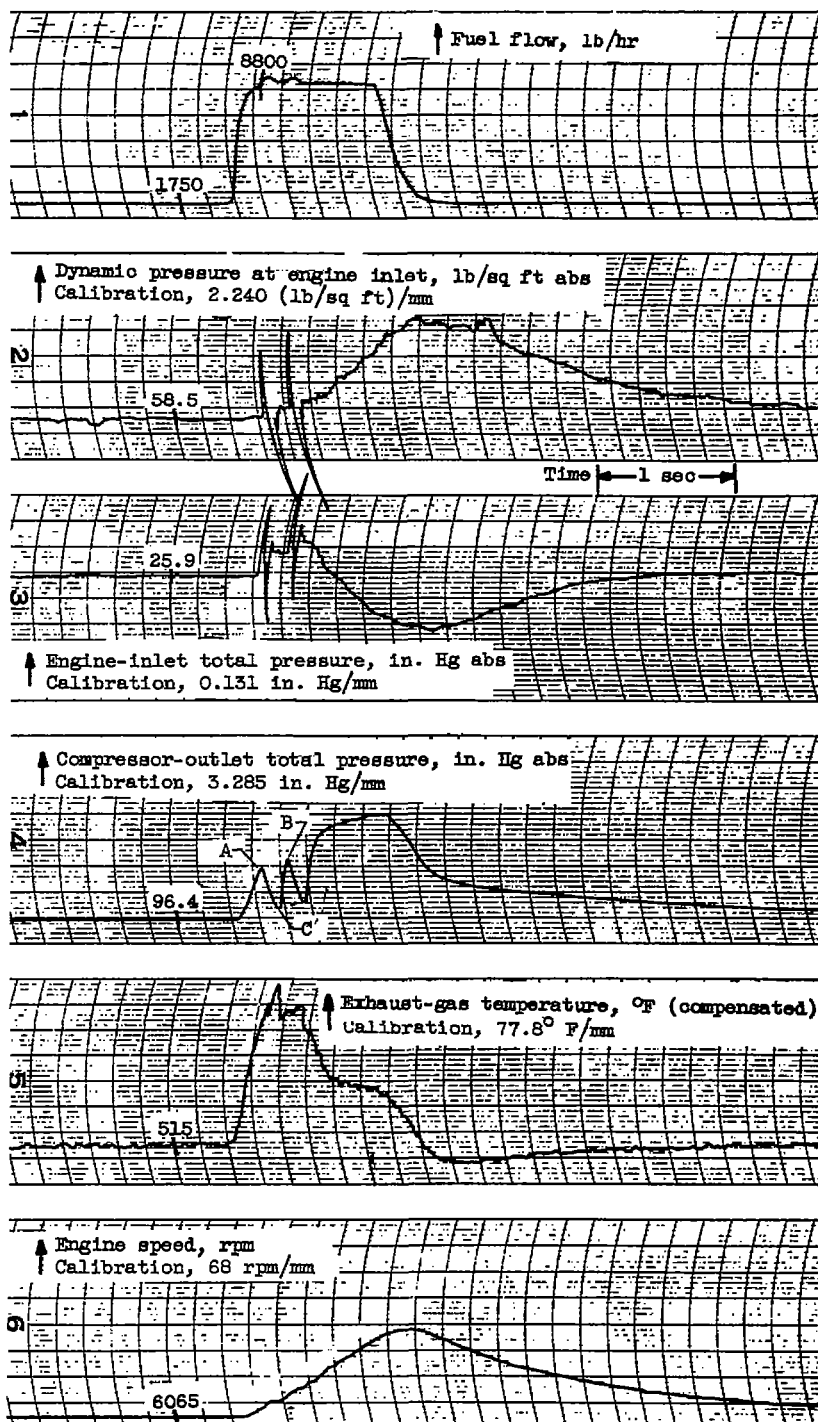
(d) Compressor efficiency.

Figure 11. - Concluded. Effect of inlet-guide-vane position on compressor operation.



(a) Encountering surge with stall. Altitude, 35,000 feet; engine-inlet air temperature,  $-10^{\circ}$  F.

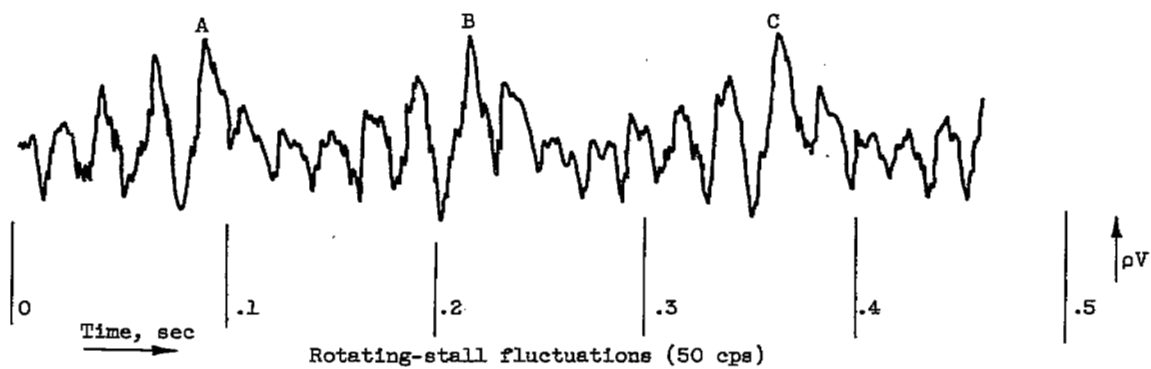
Figure 12. - Oscillograph traces of performance parameters during engine acceleration. Inlet guide vanes open; flight Mach number, 0.8.



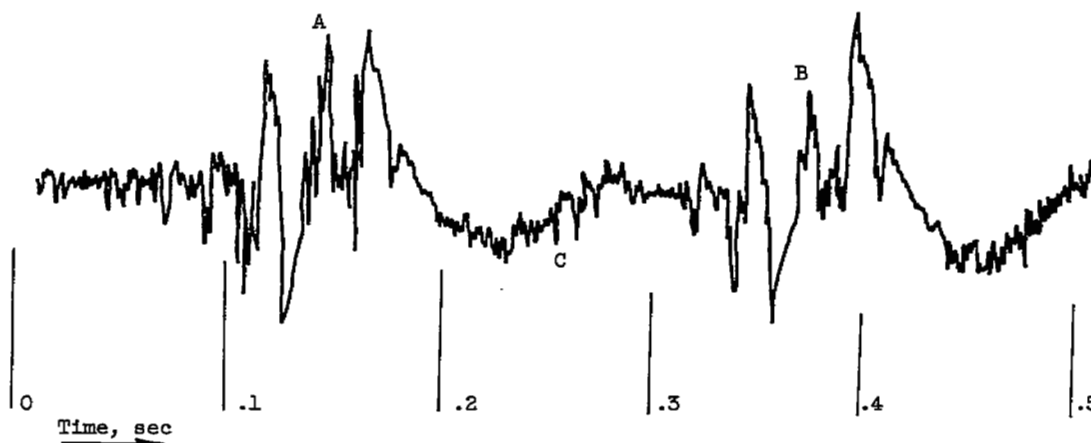
(b) Encountering surge. Altitude, 15,000 feet; engine-inlet air temperature, 43° F.

Figure 12. - Concluded. Oscillograph traces of performance parameters during engine acceleration. Inlet guide vanes open; flight Mach number, 0.8.

3494  
CZ-5



(a) Surge with stall.



(b) Surge.

Figure 13. - Oscillograph traces of hot-wire-anemometer probe during accelerations encountering two types of compressor surge.

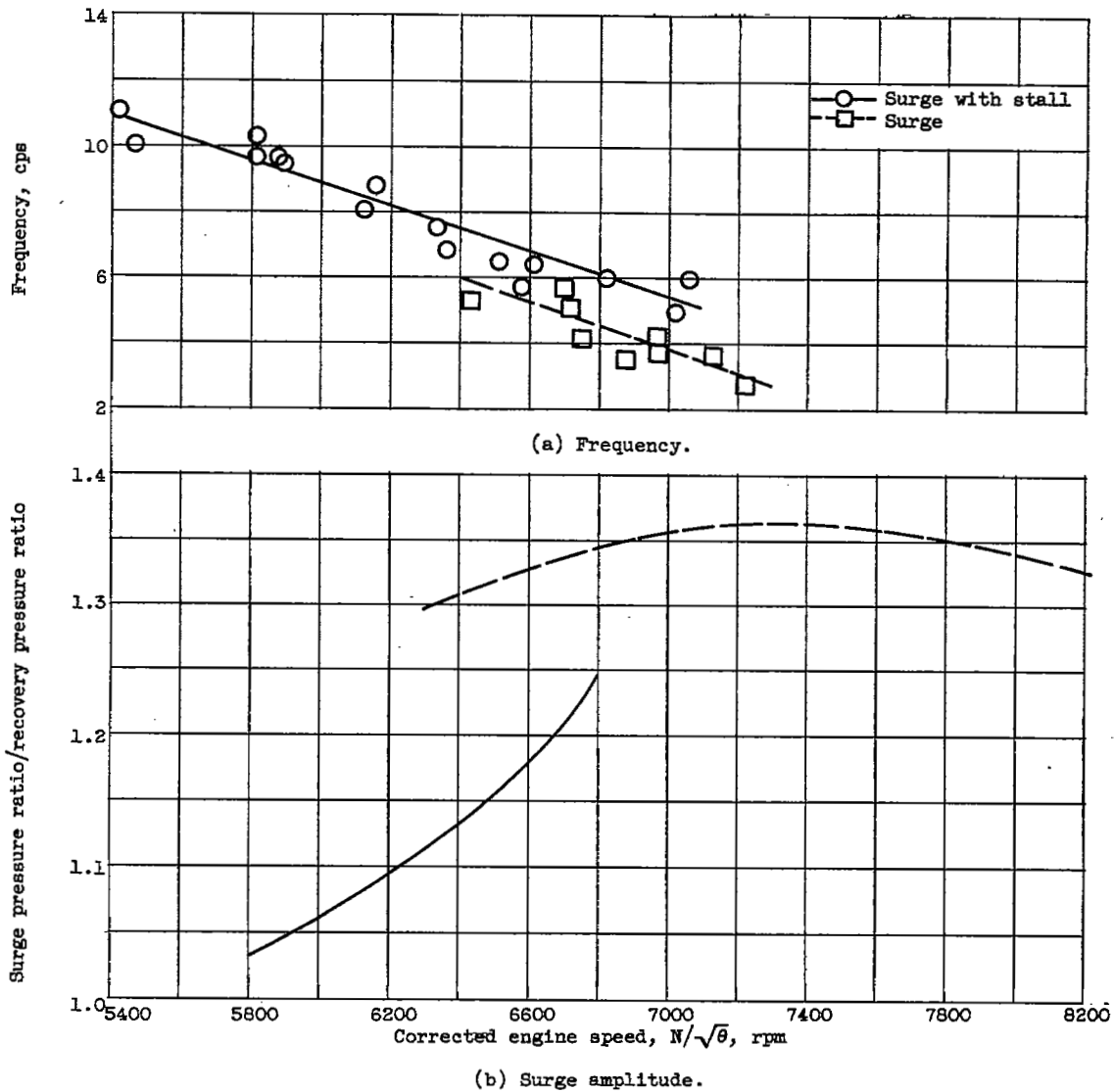
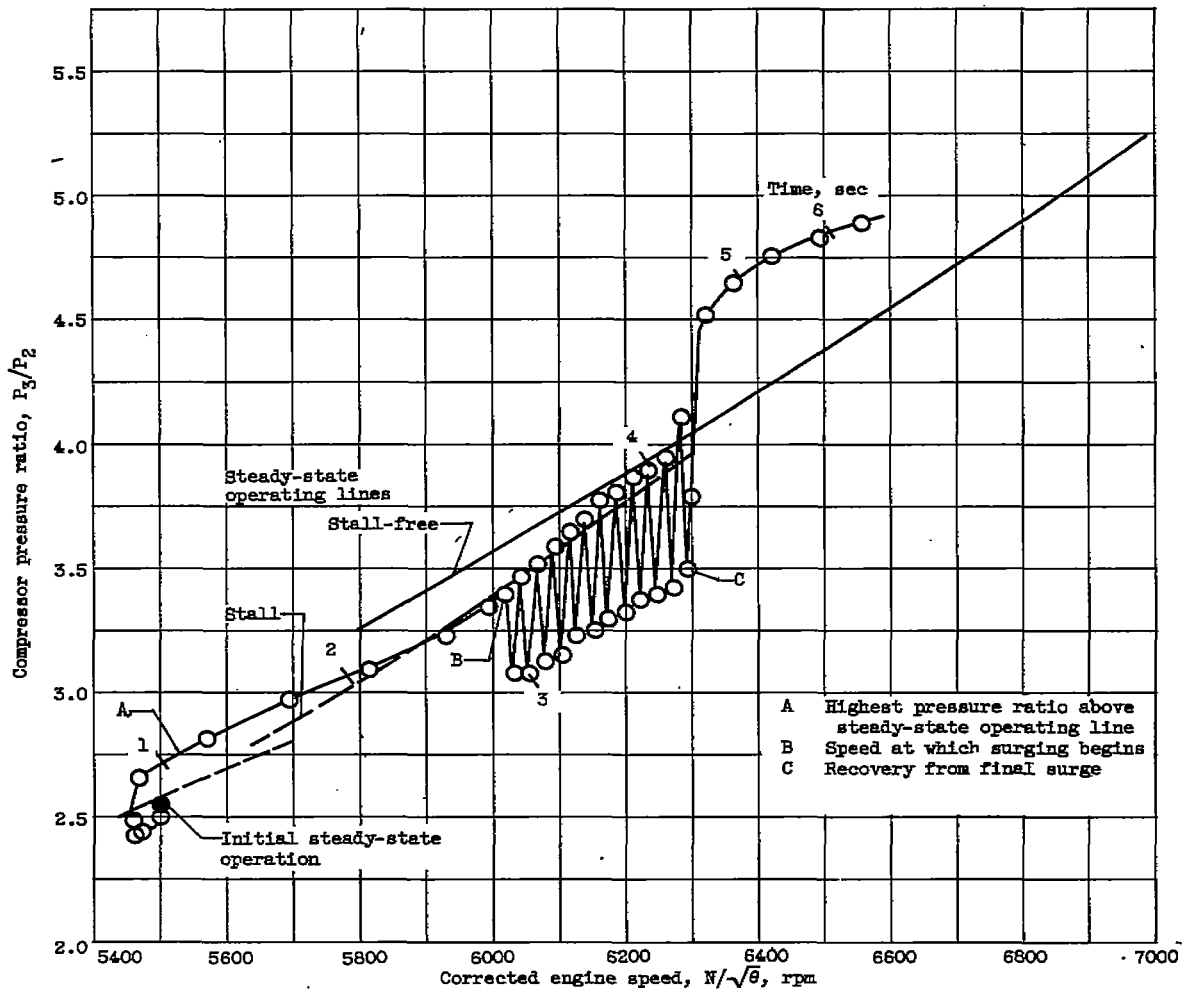


Figure 14. - Variation of frequency and surge amplitude with engine speed for two types of surge.

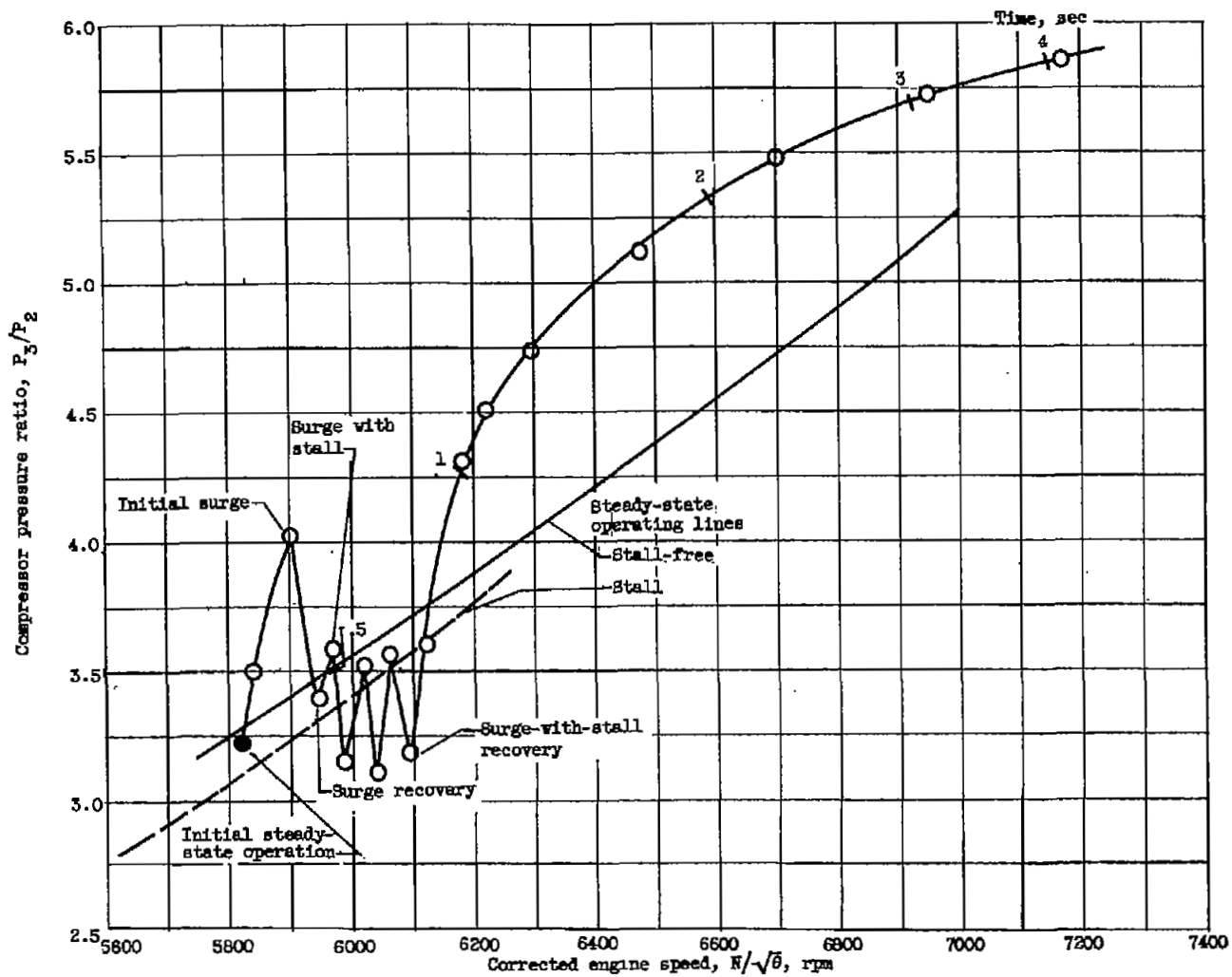
3494

CZ-5 back



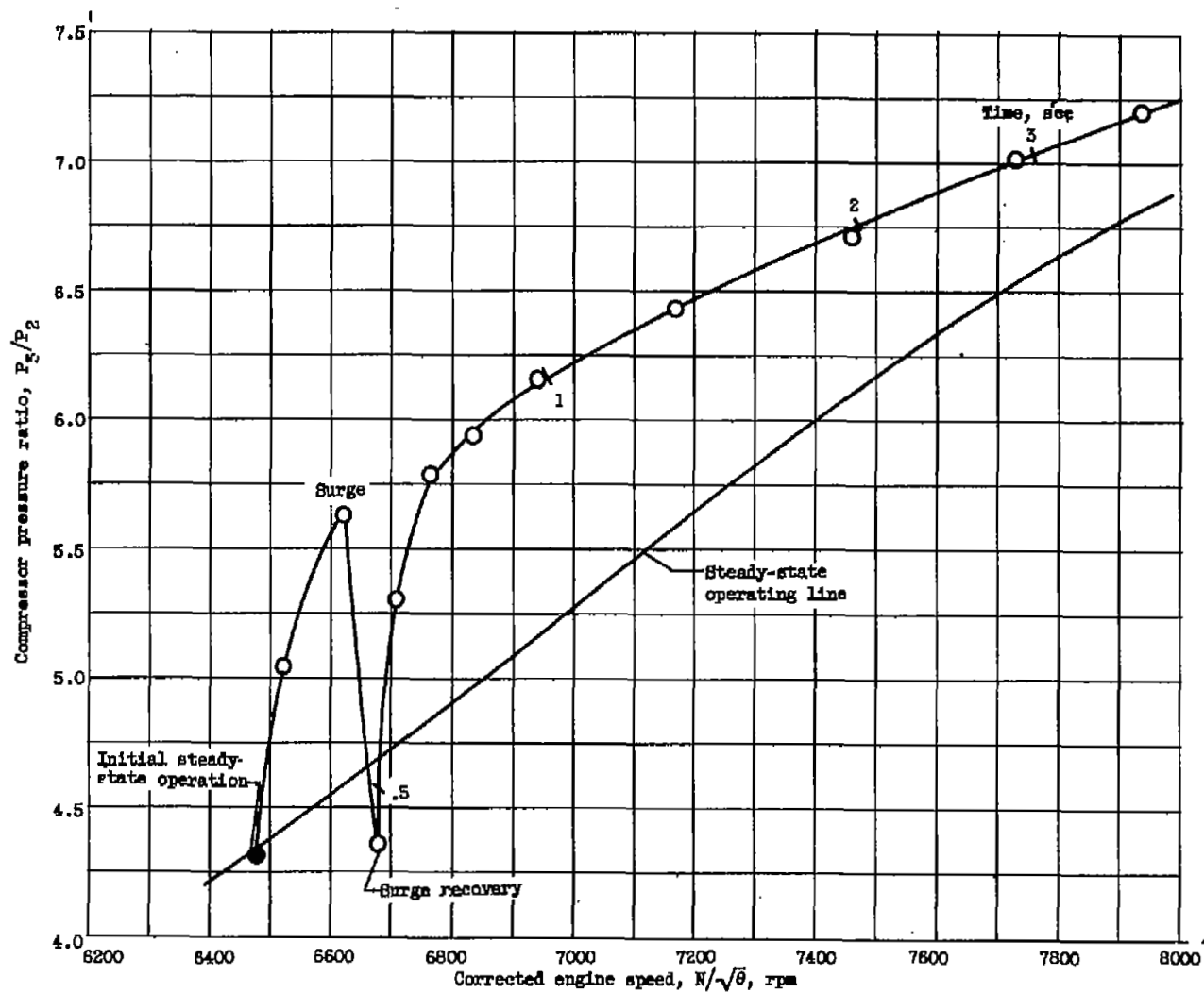
(a) Acceleration into surge with stall from steady-state operation in tip stall.

Figure 15. - Effects of acceleration with inlet guide vanes open. Altitude, 35,000 feet; flight Mach number, 0.8.



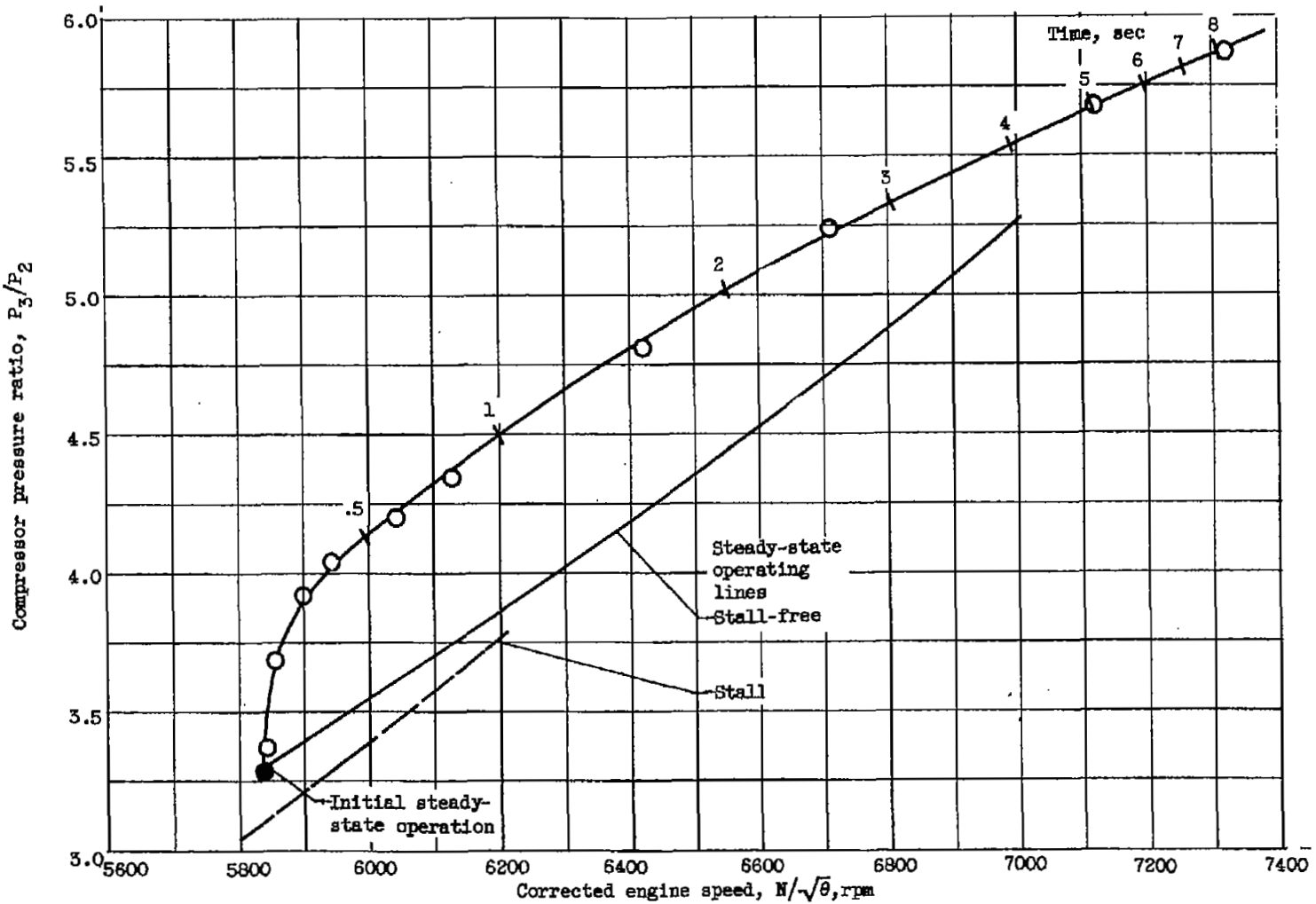
(b) Acceleration into surge and subsequent surge with stall from stall-free steady-state operation.

Figure 15. - Continued. Effects of acceleration with inlet guide vanes open. Altitude, 35,000 feet; flight Mach number, 0.8.



(c) Acceleration into surge from stall-free steady-state operation.

Figure 15. - Continued. Effects of acceleration with inlet guide vanes open. Altitude, 35,000 feet; flight Mach number, 0.8.



(d) Successful acceleration from stall-free steady-state operation.

Figure 15. - Concluded. Effects of acceleration with inlet guide vanes open. Altitude, 35,000 feet; flight Mach number, 0.8.

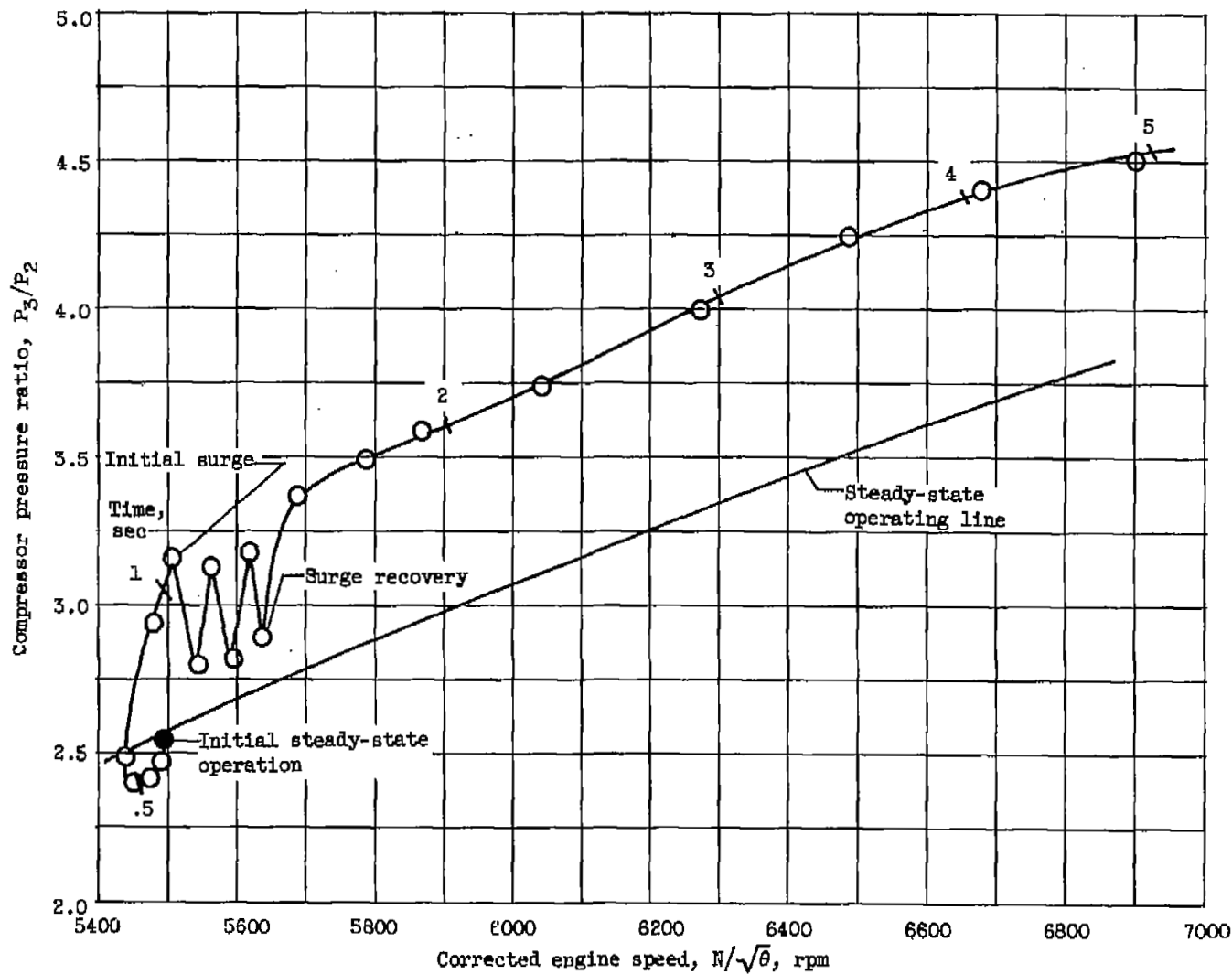


Figure 18. - Stall encountered in acceleration with inlet guide vanes closed. Altitude, 35,000 feet; flight Mach number, 0.8.

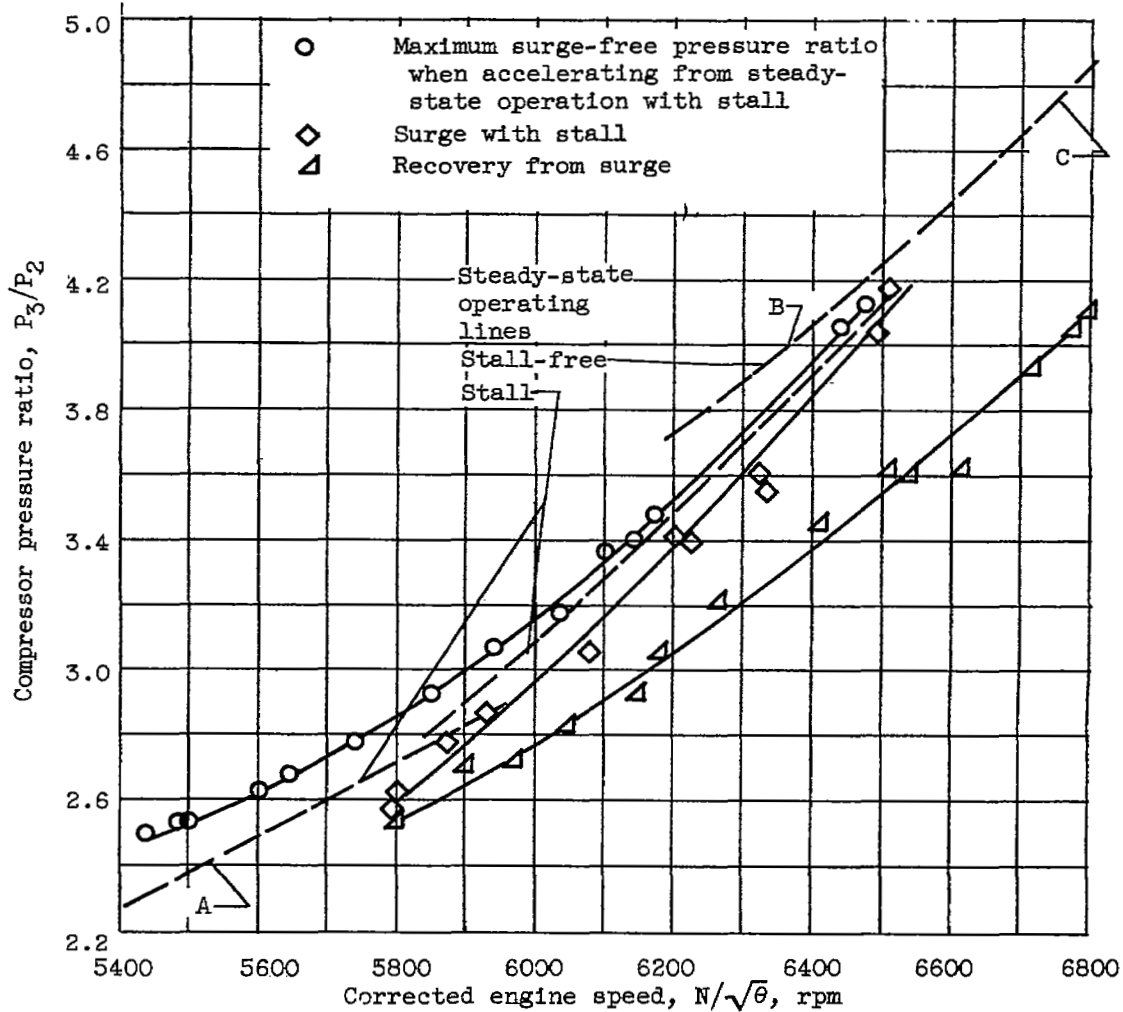
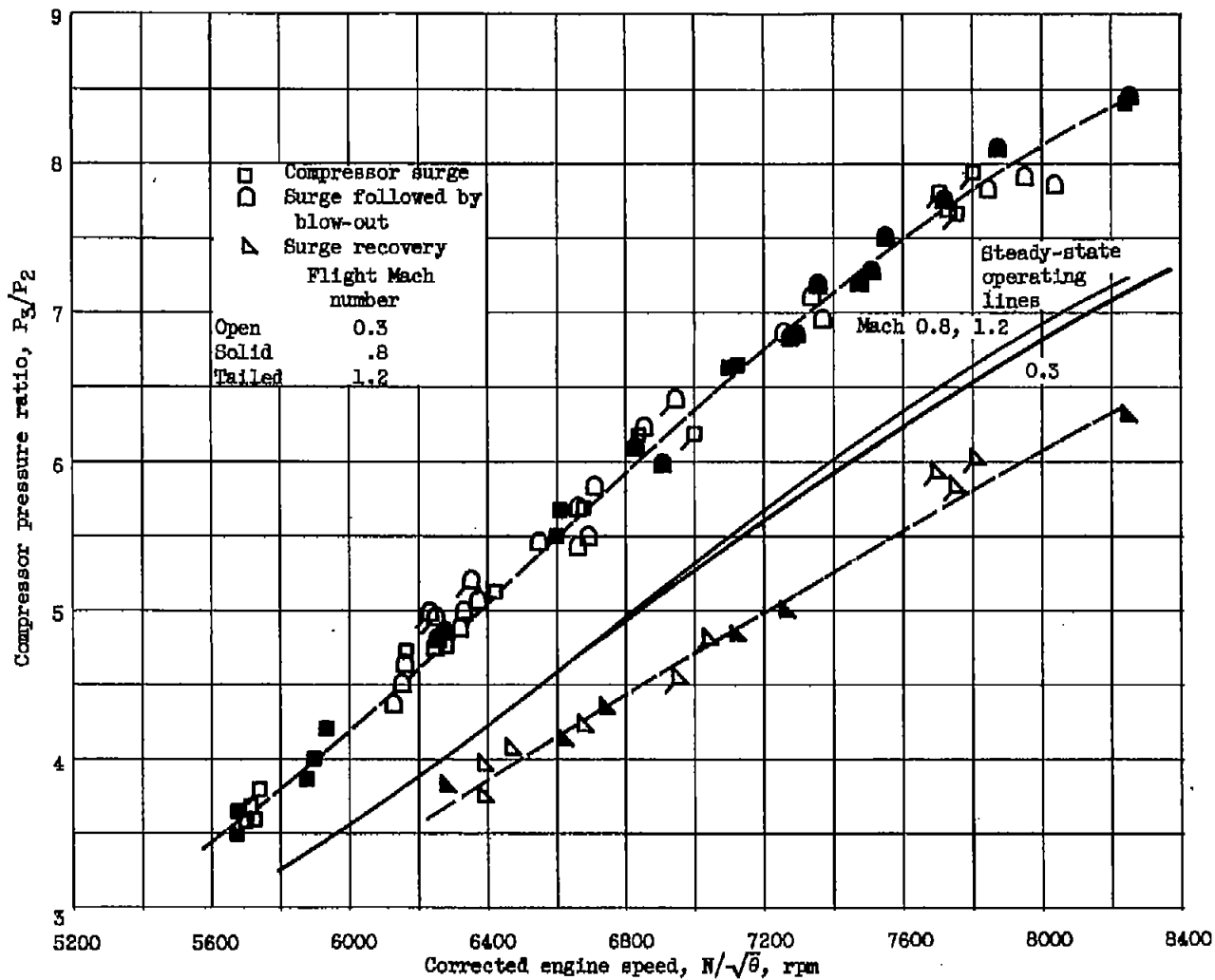
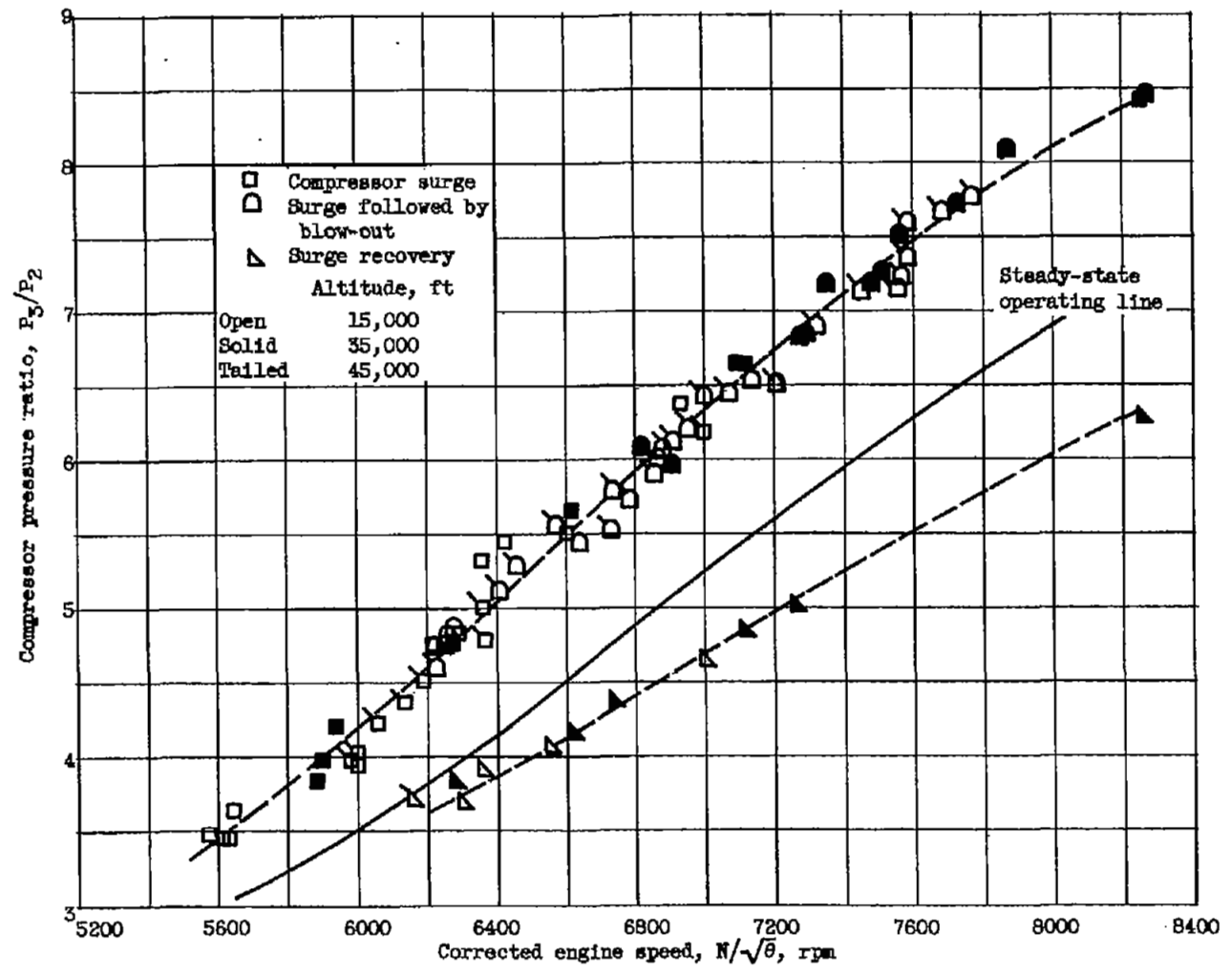


Figure 17. - Surge characteristics in steady-state stall region. Altitude, 35,000 feet; flight Mach number, 0.8. (For typical acceleration from regions A, B, and C, see figs. 15(a), (b), and (c), respectively.)



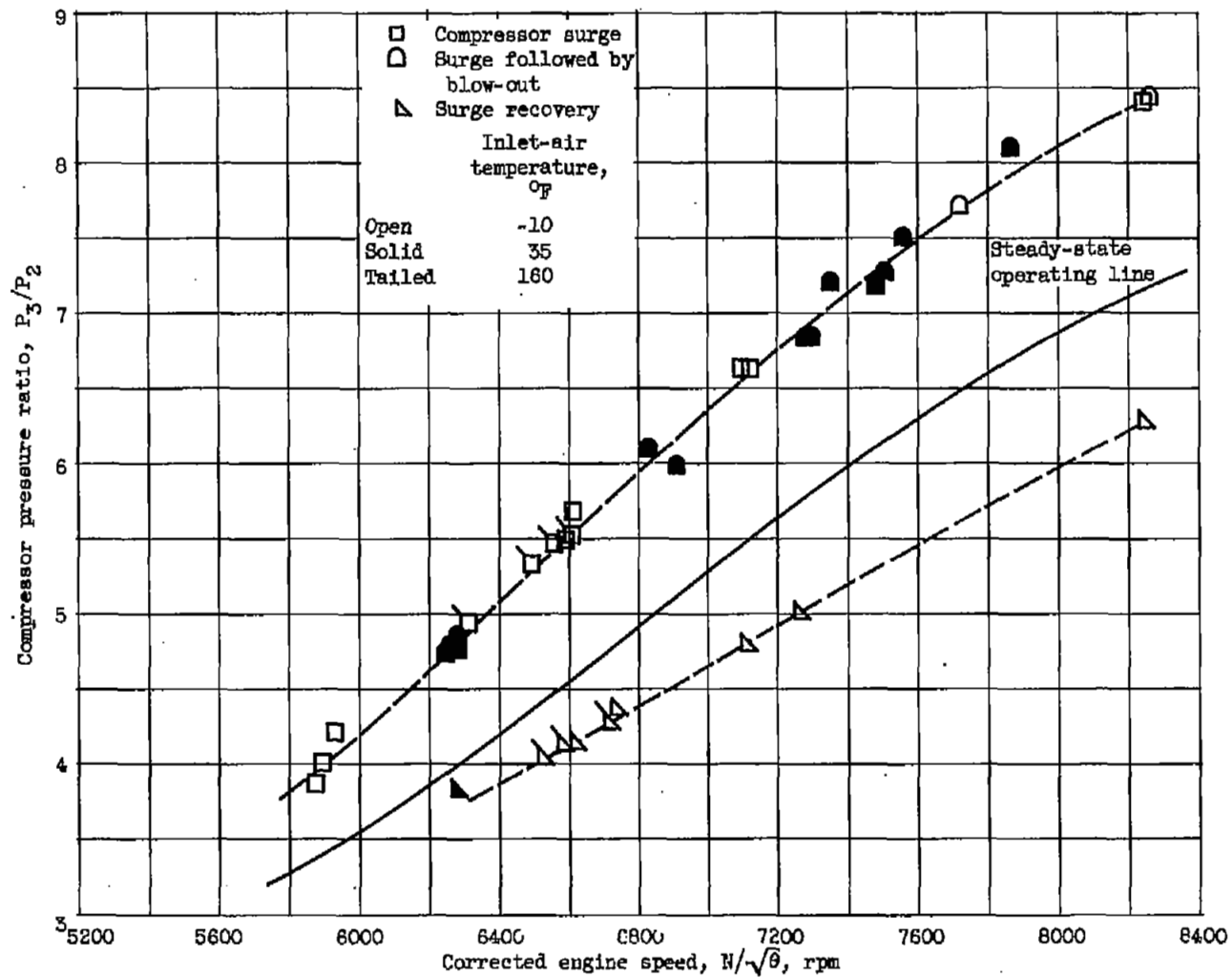
(a) Flight Mach number. Altitude, 35,000 feet.

Figure 18. - Effects of operating conditions on compressor surge during acceleration from stall-free steady-state operation. Inlet guide vanes open.



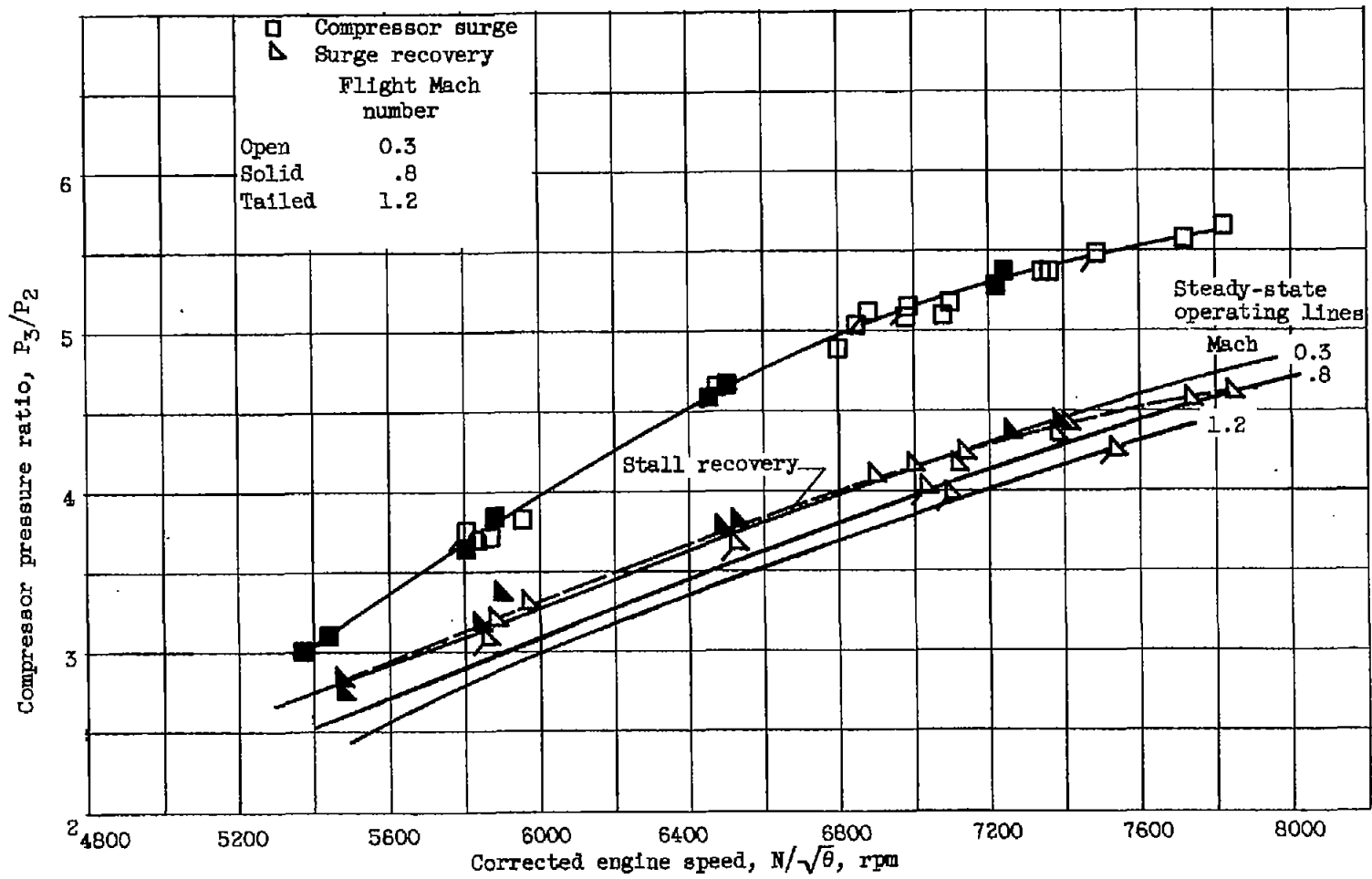
(b) Altitude. Flight Mach number, 0.8.

Figure 18. - Continued. Effects of operating conditions on compressor surge during acceleration from stall-free steady-state operation. Inlet guide vanes open.



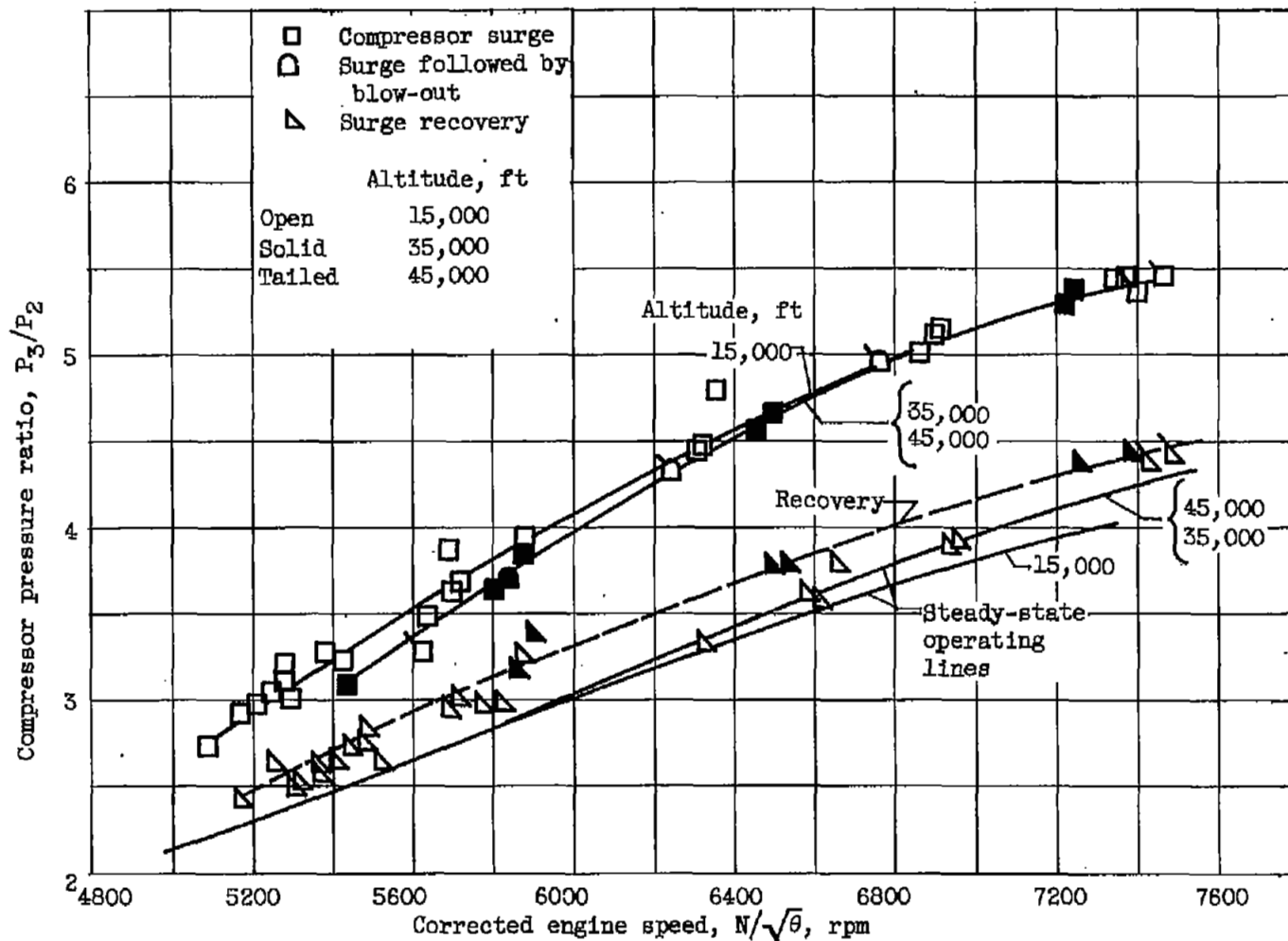
(c) Inlet-air temperature. Altitude, 35,000 feet; flight Mach number, 0.8.

Figure 18. - Concluded. Effects of operating conditions on compressor surge during acceleration from stall-free steady-state operation. Inlet guide vanes open.



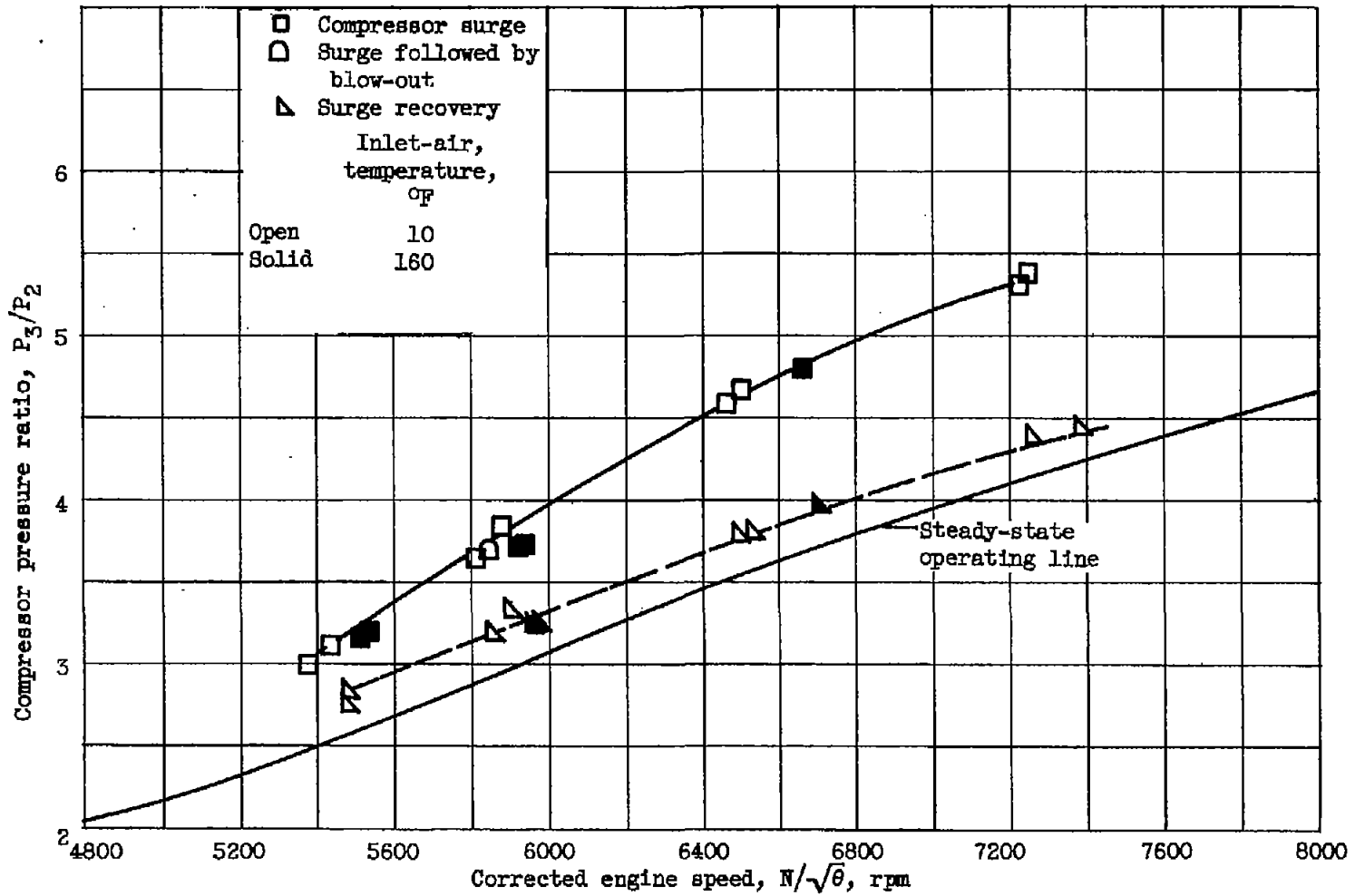
(a) Flight Mach number. Altitude, 35,000 feet.

Figure 19. - Effects of operating conditions on compressor surge during acceleration. Inlet guide vanes closed.



(b) Altitude. Flight Mach number, 0.8.

Figure 19. - Continued. Effects of operating conditions on compressor surge during acceleration. Inlet guide vanes closed.



(c) Inlet-air temperature. Altitude, 35,000 feet; flight Mach number, 0.8.

Figure 19. - Concluded. Effects of operating conditions on compressor surge during acceleration. Inlet guide vanes closed.

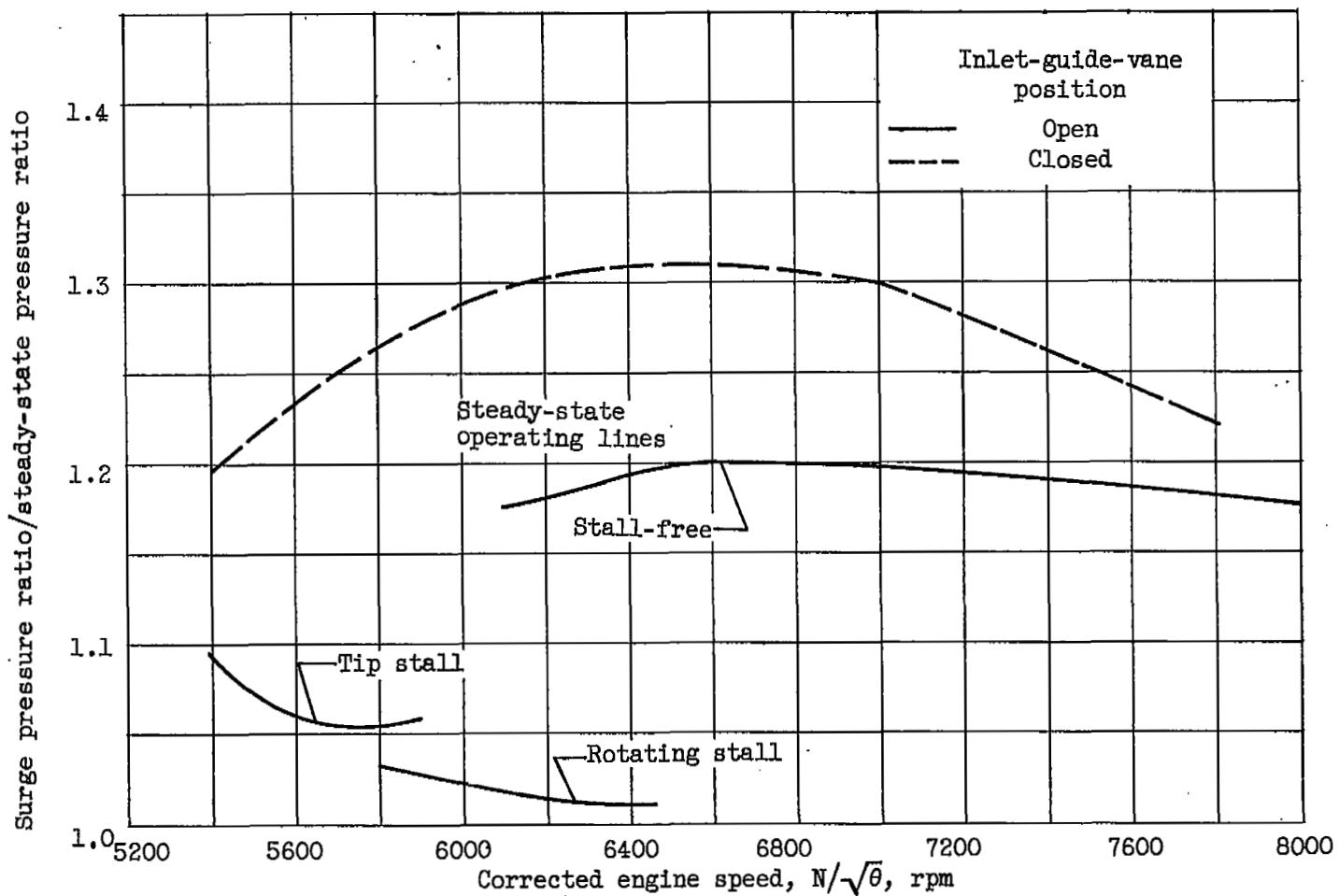


Figure 20. - Effect of inlet-guide-vane position on margin of compressor pressure ratio available for acceleration.

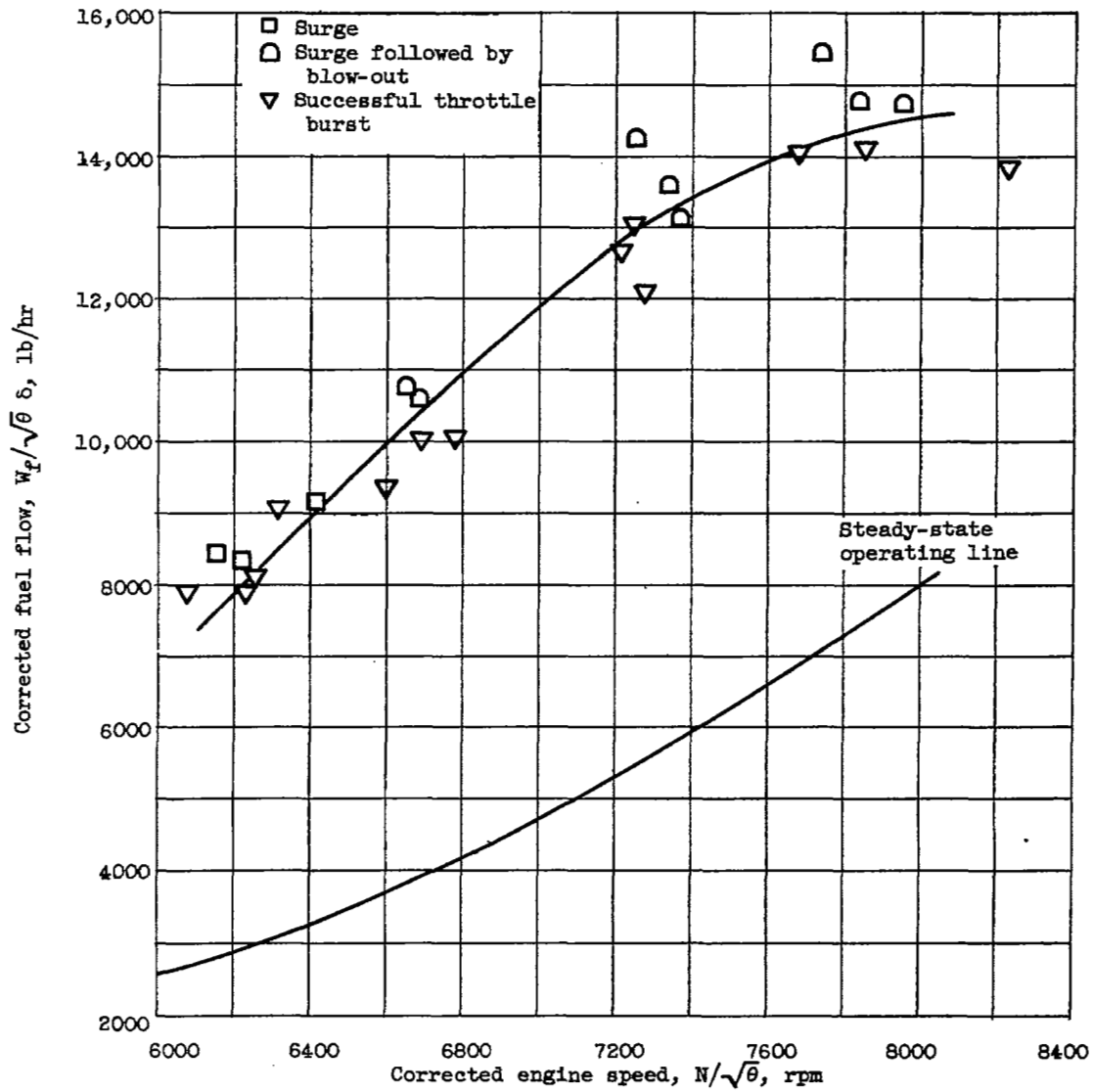
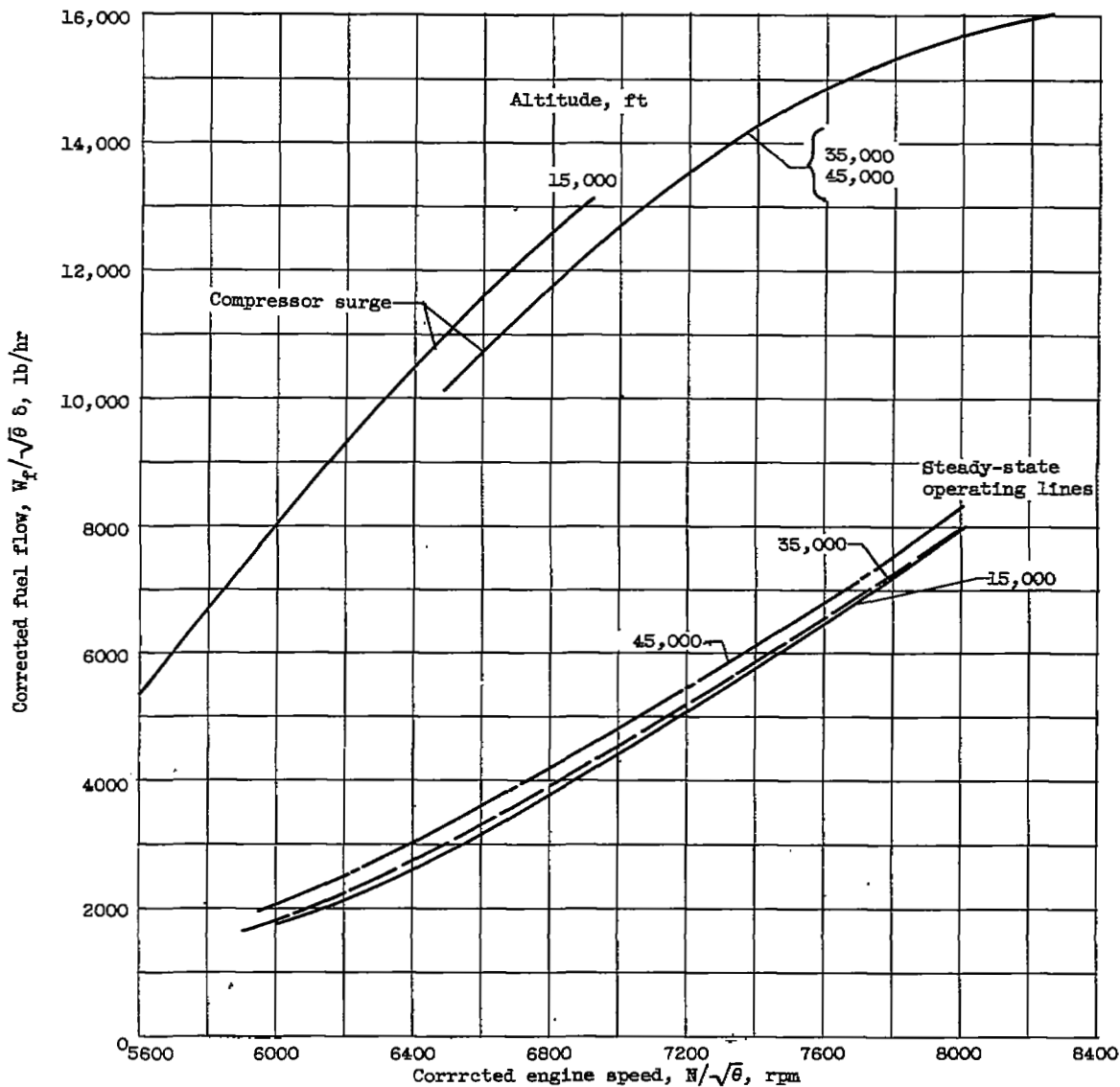


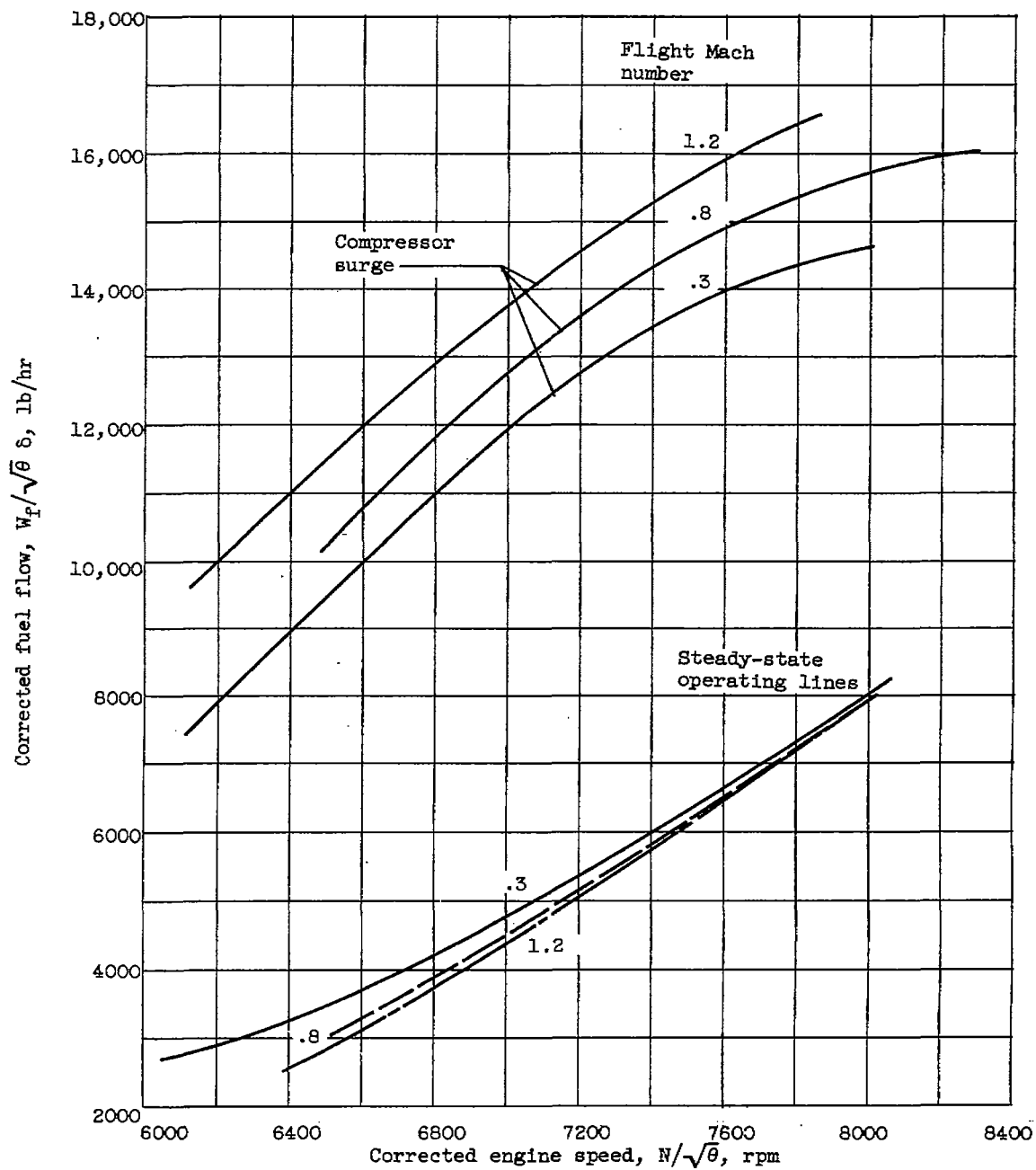
Figure 21. - Determination of engine fuel-flow surge limit. Altitude, 35,000 feet; flight Mach number, 0.3; inlet guide vanes open.

3494



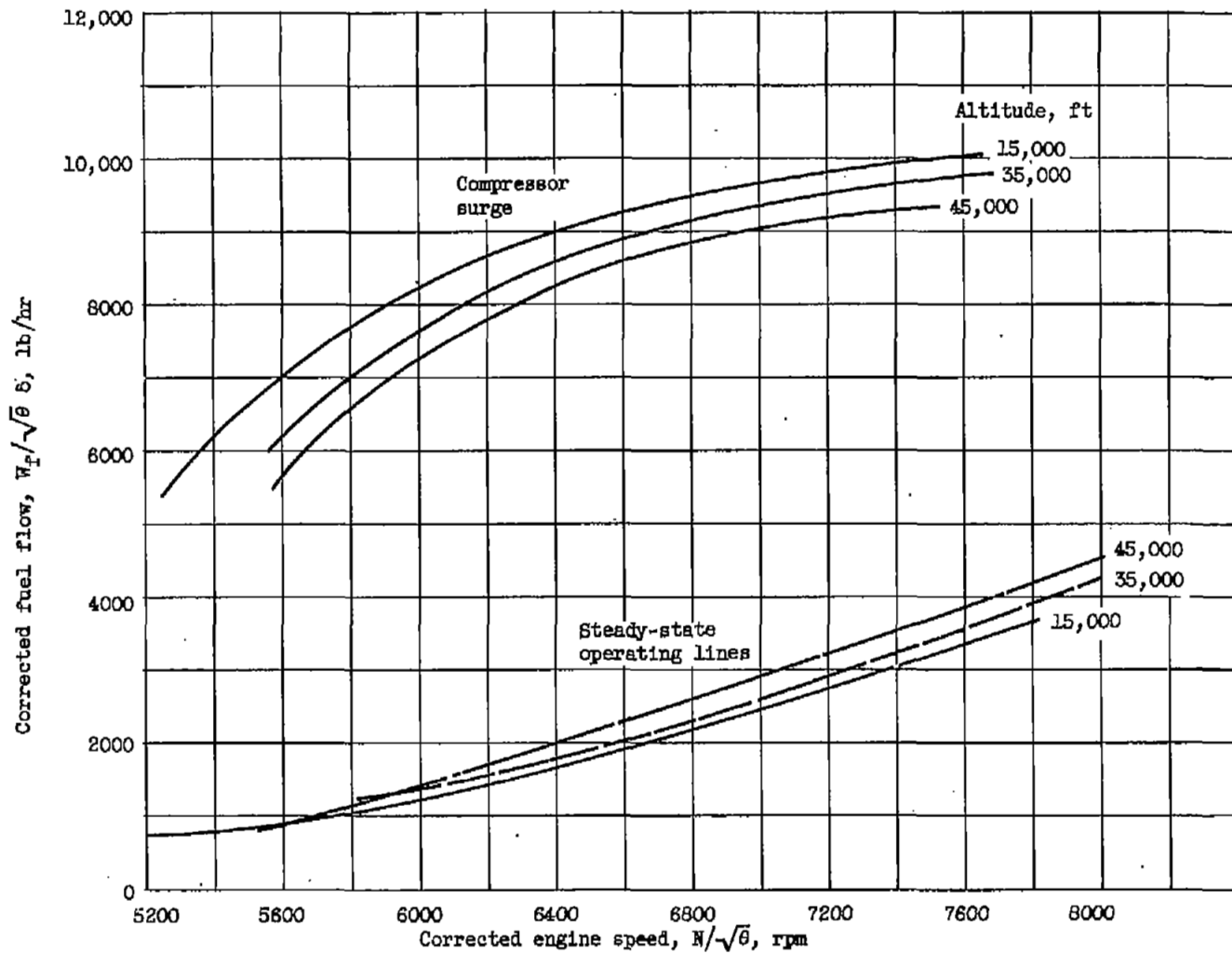
(a) Altitude. Flight Mach number, 0.8.

Figure 22. - Effect of operating conditions on fuel-flow surge lines. Inlet guide vanes open.



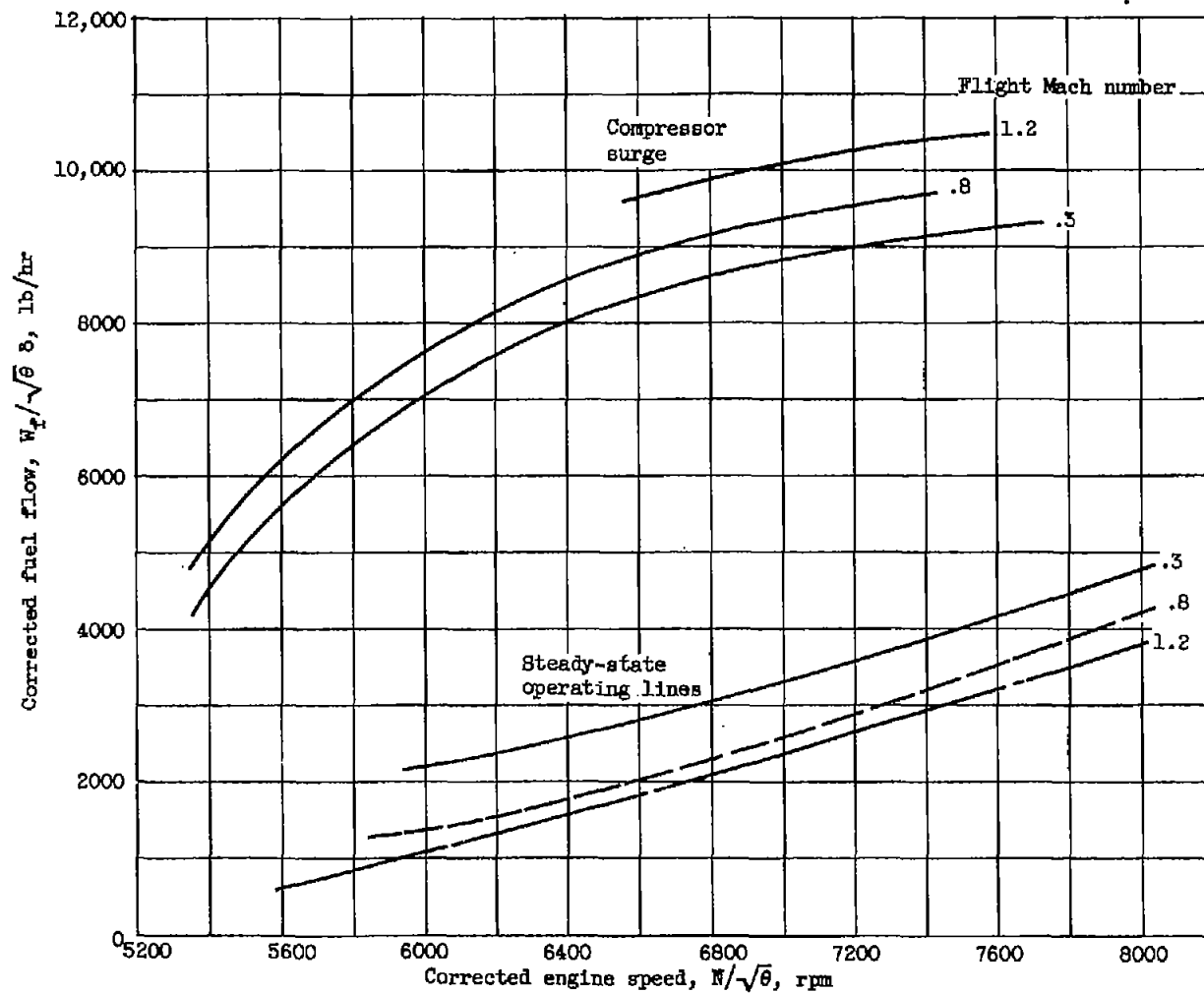
(b) Flight Mach number. Altitude, 35,000 feet.

Figure 22. - Concluded. Effect of operating conditions on fuel-flow surge lines. Inlet guide vanes open.



(a) Altitude. Flight Mach number, 0.8.

Figure 23. - Effect of operating conditions on fuel-flow surge lines. Inlet guide vanes closed.



(b) Flight Mach number. Altitude, 35,000 feet.

Figure 23. - Concluded. Effect of operating conditions on fuel-flow surge lines.  
Inlet guide vanes closed.

3494

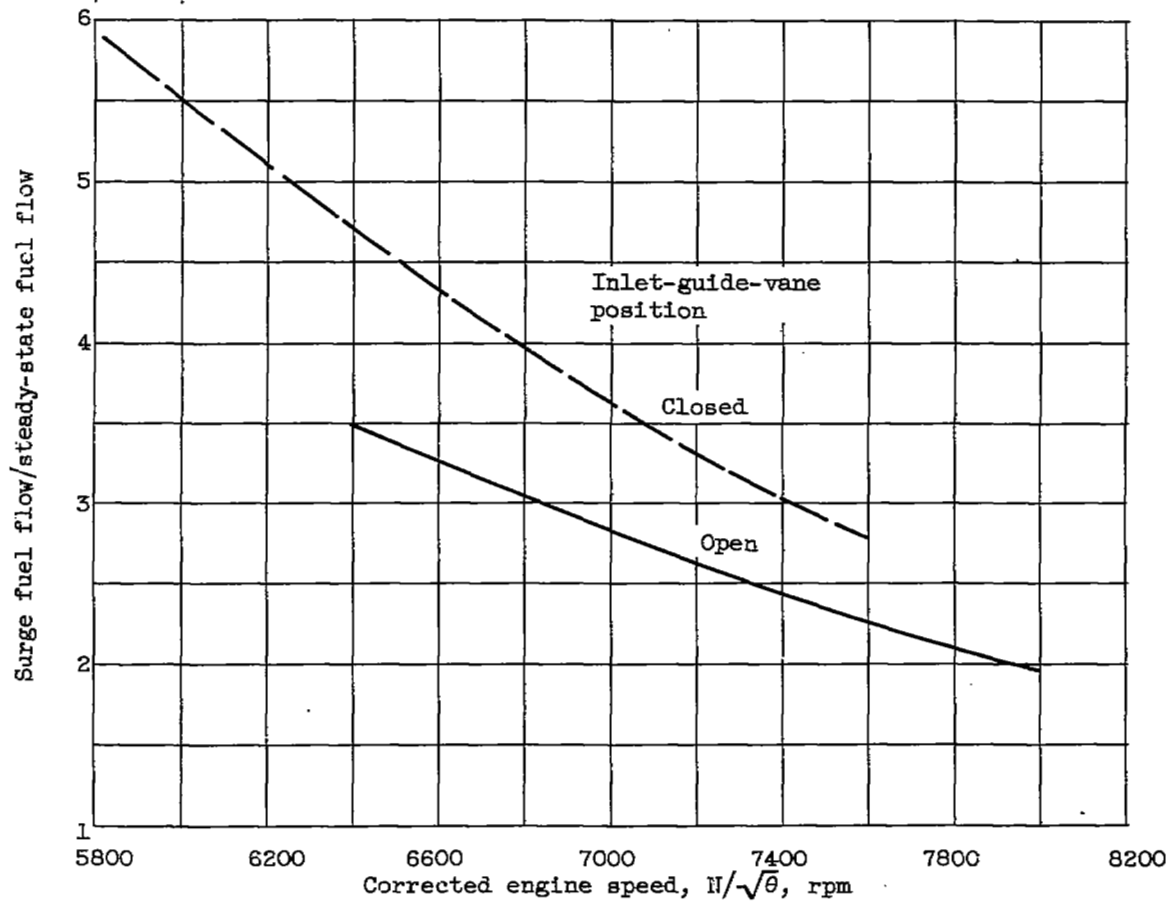


Figure 24. - Variation of fuel-flow margin available for acceleration with corrected engine speed for open and closed inlet guide vanes. Altitude, 35,000 feet; flight Mach number, 0.8.

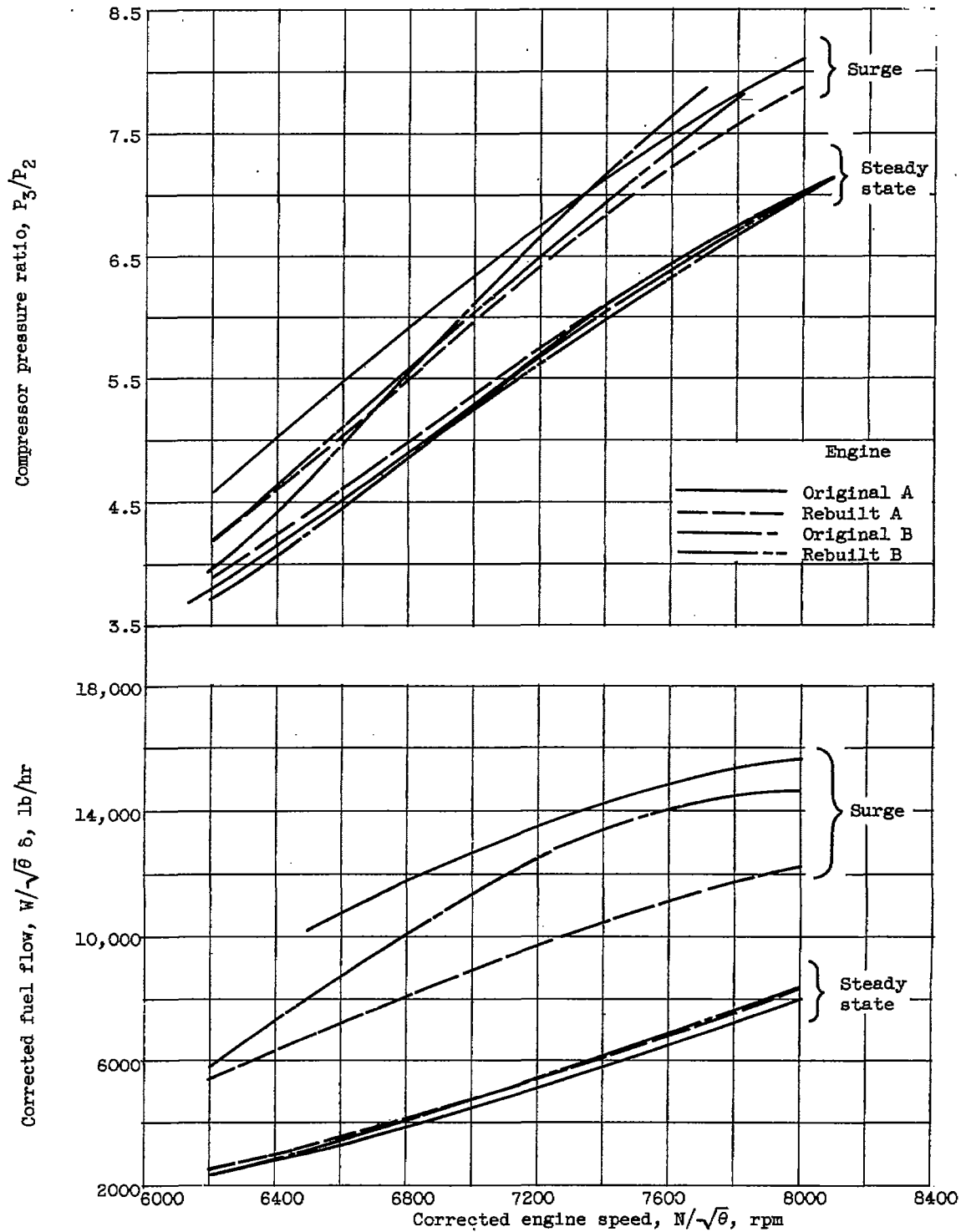


Figure 25. - Comparison of operating limits obtained from engines used in investigation.

NASA Technical Library



3 1176 01435 7413